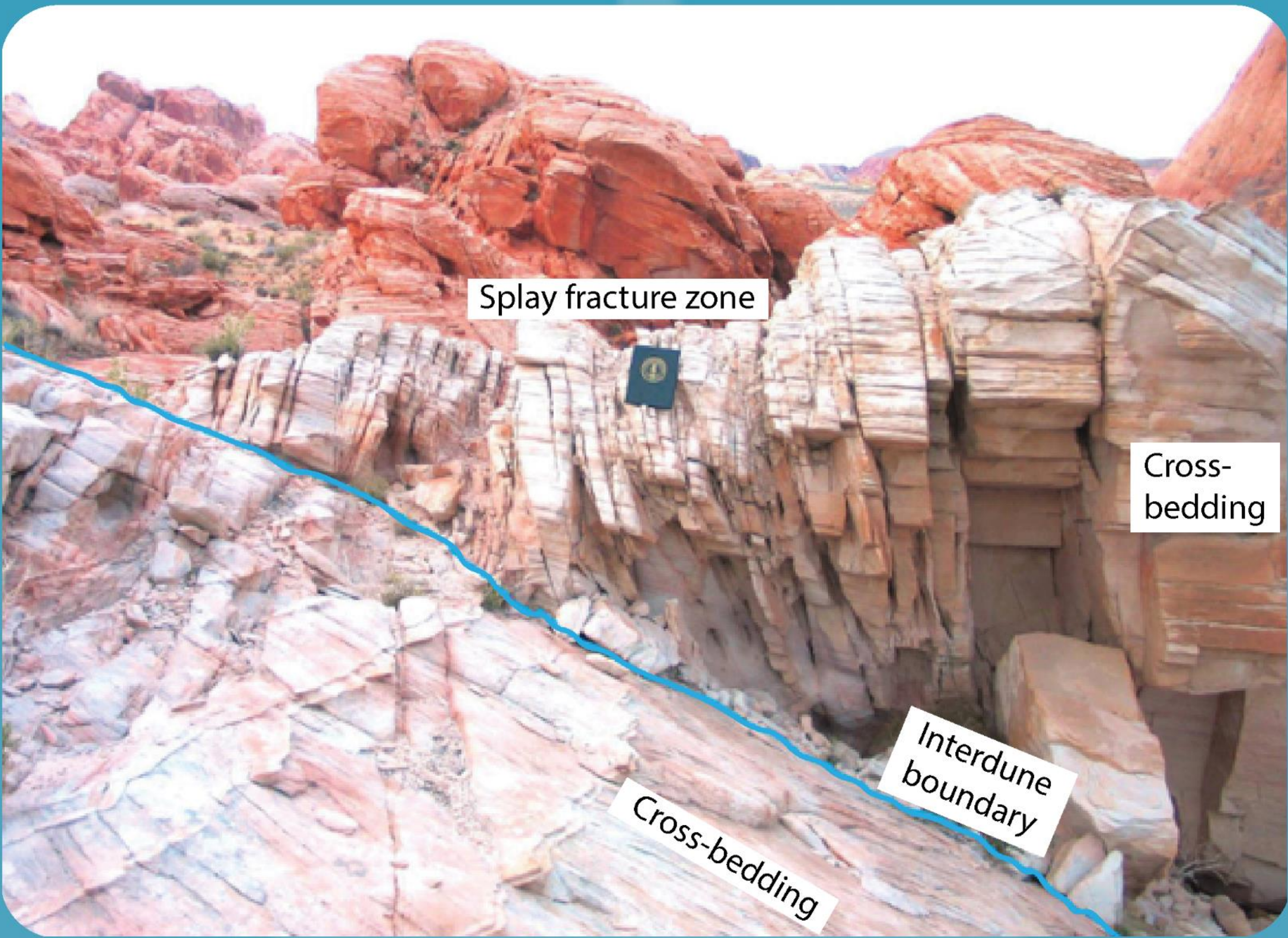

Fractures and Faults in Sandstone and Sandstone-Shale/Mudstone Sequences and Their Impact on Groundwater

Atilla Aydin, Ramil Ahmadov, Marco Antonellini, John Cherry, Antonino Cilona, Shang Deng, Eric Flodin, Ghislain de Joussineau, Beth Parker and Jian Zhong

THE GROUNDWATER PROJECT

Fractures and Faults in Sandstone and Sandstone-Shale/Mudstone Sequences and Their Impact on Groundwater

The Groundwater Project

Atilla Aydin
Professor Emeritus
Department of Geological Sciences
Stanford University
Stanford, California, USA

Ramil Ahmadov
Senior Geophysical Advisor, Manager Rock Physics, CGG and University of Houston
Houston, Texas, USA

Marco Antonellini
Associate Professor
Department of Biological, Geological and Environmental Sciences, University of Bologna
Bologna, Italy

John Cherry
Morwick G360 Institute
Guelph University
Guelph, Ontario, Canada

Antonino Cilona
Structural Geologist
Shell Global Solutions
The Netherlands

Shang Deng
Senior Engineer, Petroleum Exploration and Production Research Institute
Sinopec Research Institute
Beijing, China

Eric Flodin
Earth Science Advisor
Chevron Corporation
Houston, Texas, USA

Ghislain de Joussineau
Director of Technology & Operations
Beicip-Franlab
Paris, France

Beth Parker
Professor, School of Engineering
University of Guelph
The Groundwater Project
Guelph, Ontario, Canada

Jian Zhong
Resident Tech Mentor, Silicon Valley
Cisco Systems
San Jose, California, USA

Fractures and Faults in Sandstone and Sandstone-Shale/Mudstone Sequences and Their Impact on Groundwater

The Groundwater Project
Guelph, Ontario, Canada
Version 3, January 30, 2023

Published by the Groundwater Project, Guelph, Ontario, Canada, 2023.

Aydin, Atilla
Fractures and Faults in Sandstone and Sandstone-Shale/Mudstone Sequences and Their Impact on Groundwater / Authors (Atilla Aydin, Ramil Ahmadov, Marco Antonellini, John Cherry, Antonino Cilona, Shang Deng, Eric Flodin, Ghislain de Joussineau, Beth Parker and Jian Zhong) - Guelph, Ontario, Canada, 2023.
69 pages
ISBN: 978-1-77470-012-9
DOI: https://doi.org/10.21083/978-1-77470-012-9↗.

Please consider signing up for the GW-Project mailing list to stay informed about new book releases, events and ways to participate in the GW-Project. When you sign up for our email list it helps us build a global groundwater community. Sign up↗.

Citation: Aydin, Atilla, Ramil Ahmadov, Marco Antonellini, John Cherry, Antonino Cilona, Shang Deng, Eric Flodin, Ghislain de Joussineau, Beth Parker and Jian Zhong, 2023, Fractures and Faults in Sandstone and Sandstone-Shale/Mudstone Sequences and Their Impact on Groundwater. The Groundwater Project, Guelph, Ontario, Canada. https://doi.org/10.21083/978-1-77470-012-9↗.

THE GROUNDWATER PROJECT

Cover Image: Photograph from Atilla Aydin's personal collection, 2021.

Dedication

This book is dedicated to the memory of Atilla Aydin (August 4, 1944, to February 8, 2022). Dr. Aydin was a field geologist in the School of Earth, Energy & Environmental Sciences (Stanford Earth). He had a preternatural ability to "read" rock formations and understand geomechanics in ways that few others could. He was born and raised in Turkey and came to Stanford University in the United States for his Master and Doctorate degrees in geology under Professor Arvid Johnson in 1974 and 1978, respectively. After earning his Doctorate, he returned to Turkey to teach as an assistant professor of geology at Istanbul Technical University, which he did from 1978 to 1980. Due to the tenuous political climate in Turkey at the time, however, Aydin eventually sought to leave his homeland. He joined the Weizmann Institute of Science in Israel as a visiting scientist in 1980, then returned to Stanford for a post-doctoral fellowship from 1980 to 1981.

Aydin carved out a niche for himself co-managing with David Pollard the Stanford Rock Fracture Project industry affiliates program, through which corporate partners supported their students and research in matters of structural geology. He returned to Stanford in 1991 as an associate professor (research), was promoted in 1997 to full professor (research), and retired in 2015. The following excerpts are provided by Atilla's co-authors in honor of his memory.

Ramil Ahmadov:

Atilla introduced me to the world of field-based structural geology. Some of the most memorable moments I have experienced at Stanford University were with Atilla, either in the field chasing faults and fractures, or in restaurants sharing a glass of wine and discussing the world's "problems." Rest in peace, Hocam!

Marco Antonellini:

This book probably represents the last contribution of Atilla to geological knowledge in an effort to share his expertise with everybody. I think it is the generous side of his personality. We all have known him for his great field insights, sound scientific work and great companionship. We will miss arguing with him on the outcrops and chatting around a good meal. Goodbye, Atilla. We will never forget you.

Antonino Cilona:

Having studied deformation bands during my Doctorate, I have always looked up to Atilla, and working with him was an honor. He made me a better geologist and taught me the importance of keeping emotions separated from work. He was excited to write a book together with many of his former students. Basically, it was like closing the loop. Unfortunately, he could not see it published, but I am sure he would have been proud of it. Grazie, Atilla. Rest in peace!

Shang Deng:

I am greatly indebted to Atilla, who initiated some of the basic ideas leading to the present work. I also owe my deepest gratitude to his encouragement and support for my research and career development.

Eric Flodin:

I have many fond, but not always comfortable, memories of working with Atilla as a graduate student. Fond, comfortable memories are when we agreed on field observations and hypotheses or shared a meal and talked about family. Fond, uncomfortable memories are when we disagreed on field observations and hypotheses or debated the focus and direction of my dissertation work. I am grateful for the sum of my interactions with Atilla, which shaped me for the better, both personally and professionally. Rest in peace, Atilla. Your presence is greatly missed by your family, friends and professional colleagues.

Ghislain de Joussineau:

Atilla was a passionate and incredibly talented geologist. I was lucky to work with him and learned a lot from him. Among all his qualities, I admired his strength of will. Atilla would never give up on an idea or a project. He also never compromised quality in everything he did, whatever it took. He taught us, his students, to always engage in our activities with the highest level of implication and rigor. I took his teaching home and still use it every day. I also remember a highly educated man who was deeply interested in foreign cultures. This was reflected in the varied origin of his students. Merci, Atilla. We all miss you!

Beth Parker:

I met Atilla in 2015 through a collaborative project where our interests were characterizing the hydraulically active fracture network in a marine turbidite sandstone in a tectonically active area in Southern California. The breadth and depth of insights brought to the project by Atilla and his post-doctoral fellow Dr. Antonino Cilona created an important structural framework based on field mapping of the multi-scaled fault and fracture network for advancing the hydrogeologic conceptual model for groundwater flow and solute transport. He strongly believed in the value of field observations to inform the structural evolution and fault hierarchies across multiple scales. Knowing that future science would build on existing knowledge, he compiled the insights he gained through his life and career in the Rock Fracture Knowledgebase↗, a digital encyclopedia on rock fractures and faults, for the benefit of future generations. Our discussions about the project, people and cultures were enlightening and entertaining, and his enthusiastic pursuit of scientific insights was remarkable.

Jian Zhong:

Atilla started on this book in July 2019 and continued working on it until March 2021, just before he returned to Istanbul. The book accompanied Atilla through most of the

COVID period, when he was no longer able to go to his office or go to swim. Atilla set up new printers and scanners at his home to help him work on the manuscripts. Even though it felt never-ending at the time, working on the Groundwater Project provided a motivation to Atilla during a very difficult time and gave me chances to visit him, which I treasure much today.

Table of Contents

The Groundwater Project Foreword

At the United Nations (UN) Water Summit held on December 2022, delegates agreed that statements from all major groundwater-related events will be unified in 2023 into one comprehensive groundwater message. This message will be released at the UN 2023 Water Conference, a landmark event that will bring attention at the highest international level to the importance of groundwater for the future of humanity and ecosystems. This message will bring clarity to groundwater issues to advance understanding globally of the challenges faced and actions needed to resolve the world's groundwater problems. Groundwater education is key.

The 2023 World Water Day theme *Accelerating Change* is in sync with the goal of the Groundwater Project (GW-Project). The GW-Project is a registered Canadian charity founded in 2018 and committed to the advancement of groundwater education as a means to accelerate action related to our essential groundwater resources. To this end, we create and disseminate knowledge through a unique approach: the democratization of groundwater knowledge. We act on this principle through our website gw-project.org/↗, a global platform, based on the principle that

"Knowledge should be free, and the best knowledge should be free knowledge." Anonymous

The mission of the GW-Project is to promote groundwater learning across the globe. This is accomplished by providing accessible, engaging, and high-quality educational materials—free-of-charge online and in many languages—to all who want to learn about groundwater. In short, the GW-Project provides essential knowledge and tools needed to develop groundwater sustainably for the future of humanity and ecosystems. This is a new type of global educational endeavor is made possible through the contributions of a dedicated international group of volunteer professionals from diverse disciplines. Academics, consultants, and retirees contribute by writing and/or reviewing the books aimed at diverse levels of readers from children to high school, undergraduate, and graduate students or professionals in the groundwater field. More than 1,000 dedicated volunteers from 127 countries and six continents are involved—and participation is growing.

Hundreds of books will be published online over the coming years, first in English and then in other languages. An important tenet of GW-Project books is a strong emphasis on visualization; with clear illustrations to stimulate spatial and critical thinking. In future, the publications will also include videos and other dynamic learning tools. Revised editions of the books are published from time to time. Users are invited to propose revisions.

We thank you for being part of the GW-Project Community. We hope to hear from you about your experience with the project materials, and welcome ideas and volunteers!

The GW-Project Steering Committee

January 2023

Foreword

More than half the global population lives where there is fresh groundwater in fractured bedrock, either rock near the surface or rock aquifers beneath unconsolidated aquifers. This book, *Fractures and Faults and Sandstone-Shale/Mudstone Sequences and Their Impact on Groundwater* represents a geological perspective on this subject and is part of the larger topic of fractured rock hydrogeology. This book follows on from *Structural Geology Applied Fractured Rock Characterization*↗ (Groundwater Project book, 2023) that is a broad introduction to the origins of the fractures significant in rock hydrogeology. To gain a full understanding of what is presented in these books, the reader will need prerequisite knowledge of structural geology as provided in an introductory course or introductory textbook. Subsequent books by the Groundwater Project will focus on flow and contaminant behavior in fractures and faults.

This book about fractures and faults in sandstone and shale/mudstone sequences is important because the literature about fractured rock hydrogeology is sparse relative to unconsolidated deposits and karst and because sandstone is an important type of aquifer in many regions. This book focus on the use of visual observations of bedrock in the field for developing conceptual models about the structural features and groundwater occurrence in these features. Fractured rock is complex and boreholes for subsurface investigation are expensive. Structural geology insights from land surface observations are important to combine with information from boreholes. There is the common intuitive perception that faults are features where bulk permeability is large relative to the host rock, but in sandstone sequences this may or not be the case depending on how shale strata have been incorporated into the deformed during formation of faults, which may or may not result in restricting flow across and/ or along the faults. The nature of the faulting governs the characteristics of the joints and bedding plane fractures away from the faults.

The research conducted by the authors of this book has included sandstone and sandstone sequences in many countries, with the common factor being guiding and connecting influence of Dr. Atilla Aydin (1944 to 2022); Dr. Aydin, formerly a professor at Stanford University (1991 to 2015), was a global leader of research on the topic. Of the book co-authors, Ramil Ahmadov, Marco Antonellini, Eric Flodin and Jian Zhong were graduate students supervised by Dr. Aydin and Antonino Cilona, Shang Deng and Ghislain de Joussineau were postdoctoral scientists on his Stanford team. Drs. Cherry and Parker were collaborators with Dr. Aydin who provided their hydrogeologic expertise on the last major project involving sandstone sequences led by Dr. Aydin. The combination of expertise and experience of these authors provides readers with a unique window into fractures and faults in the groundwater context within sandstone sequences.

John Cherry, The Groundwater Project Leader

Guelph, Ontario, Canada, November 2022

Acknowledgments

We deeply appreciate the thorough and useful reviews of and contributions to this book by the following individuals:

- Thomas Doe, Principal, Golder Associates, and Affiliate Instructor, Department of Civil and Environmental Engineering, University of Washington, Seattle, United States of America;
- Fabrizio Agosta, Associate Professor, Department of Sciences, University of Basilicata, Potenza, Italy;
- Jonathan Munn, Post-doctoral Fellow, Morwick G360 Groundwater Research Institute, University of Guelph, Guelph, Canada;
- Matthys Dippenaar, Associate Professor, Engineering Geology and Hydrogeology, University of Pretoria, Pretoria, South Africa; and,
- Everton Oliveira, President of Hidroplan, Director-President of the Instituto Água Sustentável (Sustainable Water Institute), Brazil.

We appreciate the detailed suggestions of Dr. Agosta and candid critiques of Dr. Doe, along with the exercises and solutions provided by Jonathan Munn and Danilo Amendola. We are grateful for Amanda Sills and the Formatting Team of the Groundwater Project for their oversight and copyediting of this book. We thank Eileen Poeter (Colorado School of Mines, Golden, Colorado, United States of America) for reviewing, editing and producing this book.

1 Introduction

This Groundwater Project book focuses on fractures in siliciclastic rocks, primarily in sandstones and secondarily in sandstone-shale intercalations. This focus is justified by the presence of large aquifers in sandstones of western North America and other regions of the world. The premise of this book is that fractures in these rocks may impart extreme fluid flow behavior, and are therefore critical for groundwater and contaminant flow and their containment. The diagram in Figure 1 shows that fracture types are related to the mechanics and mechanisms of their formation, and in turn, this influences their properties.

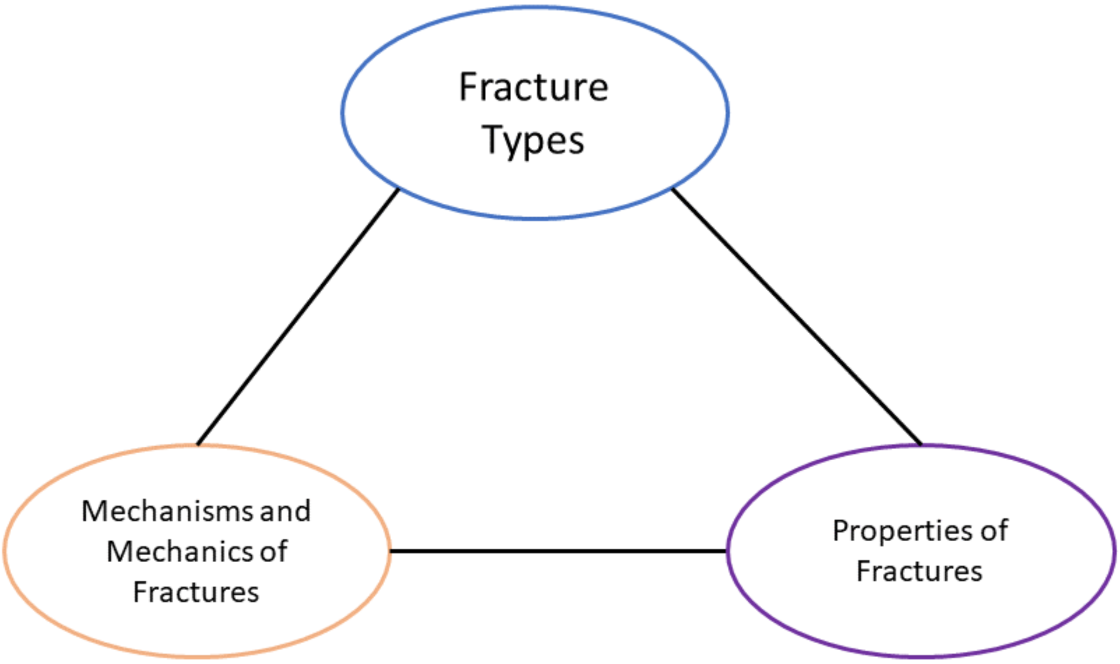

Figure 1 - Schematic diagram showing that fracture types are related to their mechanism of formation, which influences the fracture properties. Modified from Zhong and others (2009).

Fracture types that occur in siliciclastic rocks are joints, pressure solution seams (not common in the shallow crust), deformation bands and faults (Figure 2). The simplest form of each of these fracture types is a single fracture with a unique failure and formation mechanism. Although each fracture type has a wide range of physical properties, this book mainly covers the properties most relevant to groundwater science such as permeability, porosity, as well as fracture length and frequency (spatial density).

Joints
Pressure solution seams
Faults
Deformation Bands

Figure 2 - Major fracture types in siliciclastic rocks. Unlike carbonates, pressure solution seams are not common in siliciclastic rocks in the shallow crust (thus the gray color), but they are mentioned here for completeness.

Due to their variability and complex interaction with groundwater, fractures in sandstone pose a great challenge to hydrogeologists and engineers. The premise of this book is that even though remote detection methods with limited resolution are available, the direct knowledge of failure structures in siliciclastic rocks, including architecture, distribution and fluid flow properties, is effective for dealing with their impact on groundwater and contaminant flow. In natural materials, groups of fractures typically occur in a hierarchical manner, as shown in Figure 3.

Fracture zones
Fracture sets
Fracture multiple sets
Fracture assemblages
Fracture domains

Figure 3 - Common hierarchical character of fracture groups: zones, sets, assemblages and domains, which may include one or more of the individual fracture types presented in Figure 2.

Figure 4 expresses the cross-relationships among fracture types and their common distributions. This book follows an informal approach to the scheme presented by Aydin and Zhong (2017) by introducing data or information at locations in the text based on our anticipation of the needs and desires of readers with diverse interests.

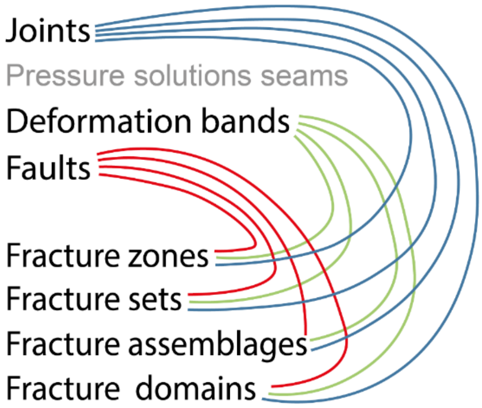

Figure 4 - Linkages between fracture types and their entities.

As an example, Figure 5 displays a gallery of pictures from the Aztec Sandstone at Valley of Fire State Park in southeastern Nevada, USA to highlight the interplay among the various fractures listed in Figure 2 and groundwater. The first image of the gallery (Figure 5a) is a series of deformation bands that compartmentalize an aeolian sandstone with extensive cross-beds trending from bottom left to top right. The image in the middle (Figure 5b) shows joints and sheared joints marked by the yellow color of precipitant materials, which is produced by water percolating along the fractures over geological time. The image on the right (Figure 5c) is an aerial photograph hundreds of meters in dimension covering several faults that exhibit left-lateral offset of the red and light-colored sandstone units for tens of meters.

Figure 5 - A gallery of images from the Jurassic Aztec Sandstone exposed in Valley of Fire State Park, Nevada, illustrating how the fractures interacted with groundwater. a) Compaction bands compartmentalize the medium with various degrees of fluid-rock interaction reactions expressed as colorful haloes that trend from lower left to upper right. These are cross-beds, many of which are over-printed by bed-parallel compaction bands. The lineaments in the direction of the viewer are compaction bands. b) Lineaments in the lower half of the view are joints and sheared joints marked by yellow infill and reaction haloes caused by percolating paleo groundwater. c) Aerial photograph showing red and bluff sandstone units offset for tens of meters by left-lateral strike-slip faults.

This book discusses fractures in siliciclastic rocks as illustrated by figures in the Introduction (Figure 1 to Figure 4), primarily focusing on fractures in sandstones and sandstone-shale sequences (Figure 5) and on their potential role in groundwater storage and flow. Each fracture type has unique formation mechanism, mechanics and properties as illustrated schematically in Figure 1. Understanding fluid flow through subsurface rocks is challenging due to the presence of a wide variety of structural and depositional heterogeneities, as recognized long ago by the pioneering work of N.G.W. Cook and his former colleagues and students at the University of California, Berkeley. On the other side of the San Francisco Bay, at Stanford University, D.D. Pollard, in partnership with A. Aydin and former members of the Stanford Rock Fracture Project, advanced knowledge of the nature and formation of rock fractures in a variety of lithologies and tectonic settings, as well as their impact on fluid flow. The material forming the backbone of this book is from the latter efforts. In this sense, the present book constitutes a Stanford-centric view of rock fractures.

To make the most relevant concepts and illustrations accessible to the readers, some details are provided in boxes at the end of this book, with links to the boxes at appropriate locations throughout the book.

Those who would like to read more on topics of interest may go to the original scientific journals and online publications referenced in this book, and to the Rock Fracture Project and Shale Smear Project data repositories at the Brenner Earth Science Library, Stanford University↗.

2 A Simple Way of Defining and Recognizing Common Fracture Types

A simplified representation of the kinematics of fracture types is illustrated in Figure 6. This follows more or less the displacement discontinuity concept of S.L. Crouch (1976) of the University of Minnesota.

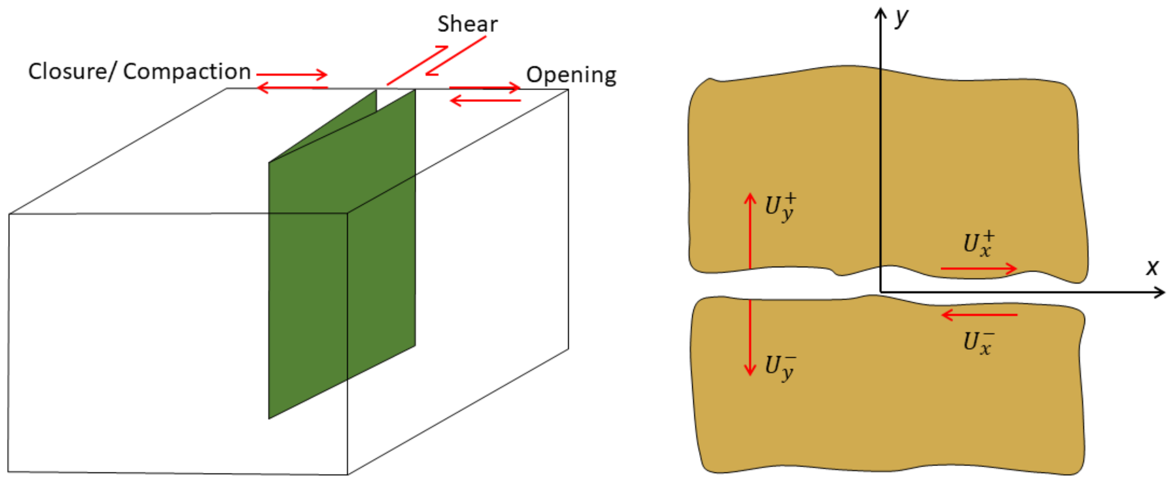

The basic kinematics include dilation opening, compaction or closure, and shear.

Positive displacements along the faces causing open aperture when positive, closed aperture when negative, and shear when parallel to the discontinuity.

Figure 6 - Left: Schematic diagram showing basic kinematics of fractures. Full arrows indicate dilation/opening and compaction/closure, and half arrows indicate shear. Right: The displacement discontinuity concept of S.L. Crouch (1976) is based on displacements of adjacent points on the two faces of a fracture, the difference of which defines the displacement discontinuity. Displacements along each face may be assumed to be positive in the positive coordinate directions. Then, displacement discontinuity normal to the fracture $D_n = U_y^+ - U_y^-$ defines opening if positive and closing if negative. Displacement discontinuity parallel to the fracture $D_s = U_x^+ - U_x^-$ denotes shear displacement discontinuity. Modified from Crouch (1976).

The three major fracture kinematics are defined as opening mode fractures (joints), closing mode fractures (pressure solution seams and compaction structures) and shearing mode fractures (shear fractures or faults). What is listed as deformation bands in Figure 2 and Figure 4 is a particular structure type formed by a unique mechanism of localization of deformation into narrow bands in the three kinematics mentioned earlier: dilation bands (opening), compaction bands (closing) and shear bands.

3 Joints

The photograph in Figure 7 shows nearly vertical joints in sandstone beds. The pencil parallel to flat-lying bedding is included to provide scale.

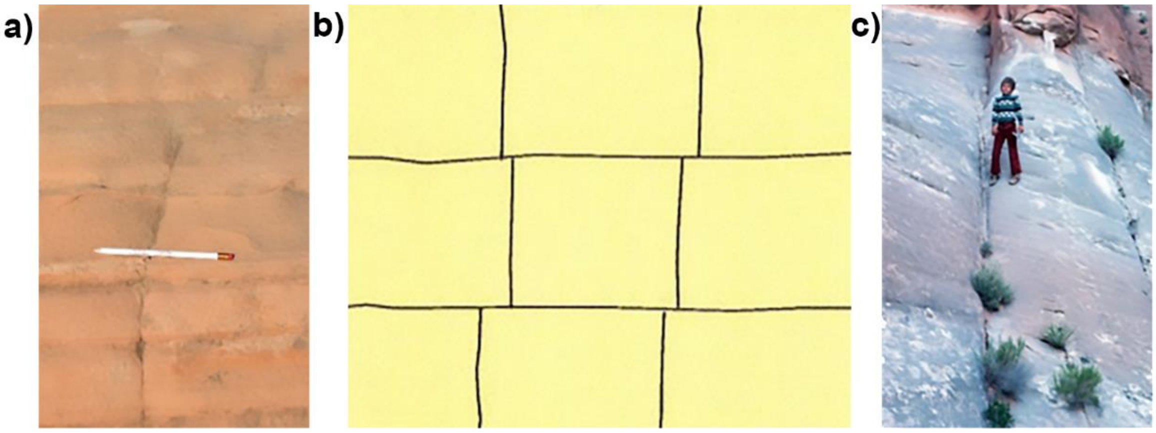

Figure 7 - a) A joint in aeolian sandstone, commonly perpendicular to beds. The pencil along the bedding interface is for scale. b) A field diagram showing joint segments confined within beds indicating the truncation or abutting at bedding interfaces. c) A steep erosional surface showing joints and sheared joints in Entrada Sandstone, northwest of the Devil's Garden parking lot, Arches National Park, Utah. Nils Johnson when he was about 8 years old appears for scale.

Joints are generally planar elements made by subparallel fracture walls that moved predominantly away from each other, resulting in an aperture value that might vary across the fracture. The field map in Figure 7b is a sketch depicting joints on an erosional surface of an outcrop with sub-horizontal layers, as in the photograph in Figure 7a. Natural joints, at least initially, commonly form orthogonal to bedding and are bed-confined (Figure 7). Bed confinement is due to truncation or abutting of joints at bed interfaces, or against any other pre-existing discontinuity, impeding the propagation of joints across (Helgeson and Aydin, 1991; Pollard and Aydin, 1988). Figure 7c shows a photograph of a steep erosional surface with a few well-developed lineaments that are joints in Jurassic Entrada Sandstone at Arches National Park, Utah, USA. The small boy in view is the younger son of A.M. Johnson, one of the pioneers of geomechanics, who along with his students studied these joints (Dyer, 1983; Cruikshank and Aydin, 1995). This site will be used later when introducing joint sets, the spacing of joints in a set and the shearing of fractures originally formed in opening mode. Often, once formed, joints are subsequently sheared and accommodate small shear offsets, the amount and kinematics of which may vary from location to location (Figure 7). Joints, if not filled by relatively strong material (in which case they are known as veins), are generally planes of weakness in rocks and are often prone to shearing. The products of this shearing are called sheared joints or simply small faults.

Aside from the aperture values, other features indicate opening across joints. These are known collectively as plumose structures, which are characteristic ornaments of joint surfaces including rib marks (Figure 8a) and hackle marks (Figure 8b). Rib marks represent pauses in the advance of the main fracture. Hackle marks are lineaments on joint surfaces that are easy to identify. Hackle marks indicate local propagation direction and, in some cases, the relative magnitude and position of the driving principal stress with respect to the axis of symmetry in the plumose pattern. These are well known in structural geology textbooks and are included here to complete the treatment of the subject for the benefit of those in allied fields.

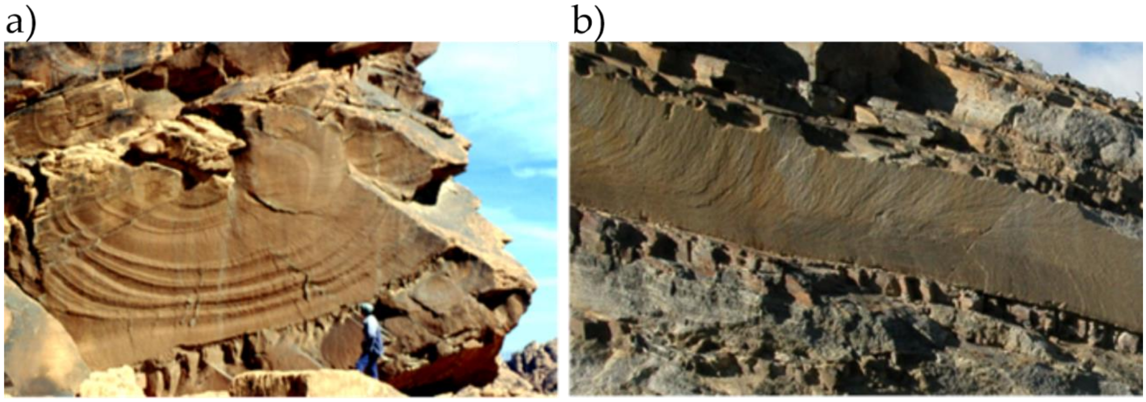

Figure 8 - Joint surface morphologies, known as plumose structures, indicate opening or dilation perpendicular to the discontinuity when it first formed. a) Rib marks in Aztec Sandstone, Valley of Fire State Park, Nevada, USA. b) Hackle marks in a siltstone layer in Chilean Patagonia. Hackle marks can be used to infer the initiation and propagation direction of the joints as well as the symmetry of the driving stresses.

4 Shear Fractures or Faults

Shear fractures or faults may be identified by the presence of offset marker horizons across the fracture (Figure 9a), which were continuous before the shearing motion. These offsets or displacements indicate relative movement of the fracture walls predominantly parallel to the fault planes. In layered rocks, faults cut and displace marker horizons as shown in the sketch. Shearing across fractures can also be identified by the presence of the so-called splay fractures as shown in Figure 9b. In this case, the motion indicated by half arrows occurred along the apparent dip direction of the discontinuity.

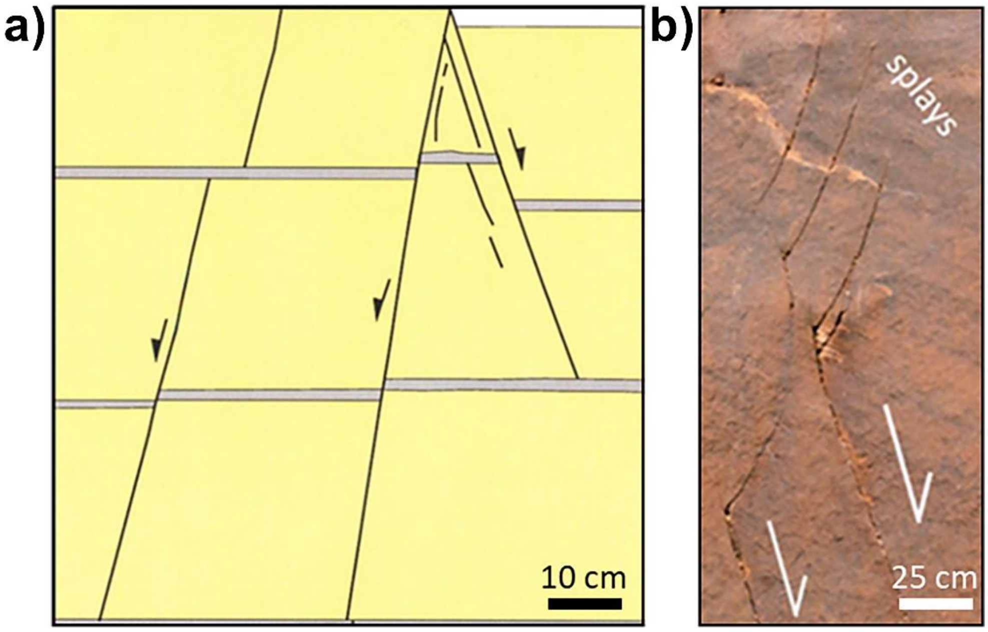

Figure 9 - a) Schematic field diagram illustrating that two marker beds (gray) are offset a few centimeters by small faults. The faults have no free ends meaning that they are vertically limited by interfaces between consecutive beds. b) Shearing of a series of discontinuities along the apparent dip direction marked by half arrows and the associated splays at the extensional quadrants above their free ends. Splay fractures can be used to infer shearing on the inclined fractures and to determine the direction of slip. Aztec Sandstone exposed at Valley of Fire State Park, Nevada, USA.

Faults have characteristic surface morphology, such as nearly planar surfaces with polished appearance (Figure 10a) and striations and grooves (Figure 10b), which are a series of lineaments on fault surfaces formed in the direction of slip. These elements are typically referred to as slickensides in structural geology.

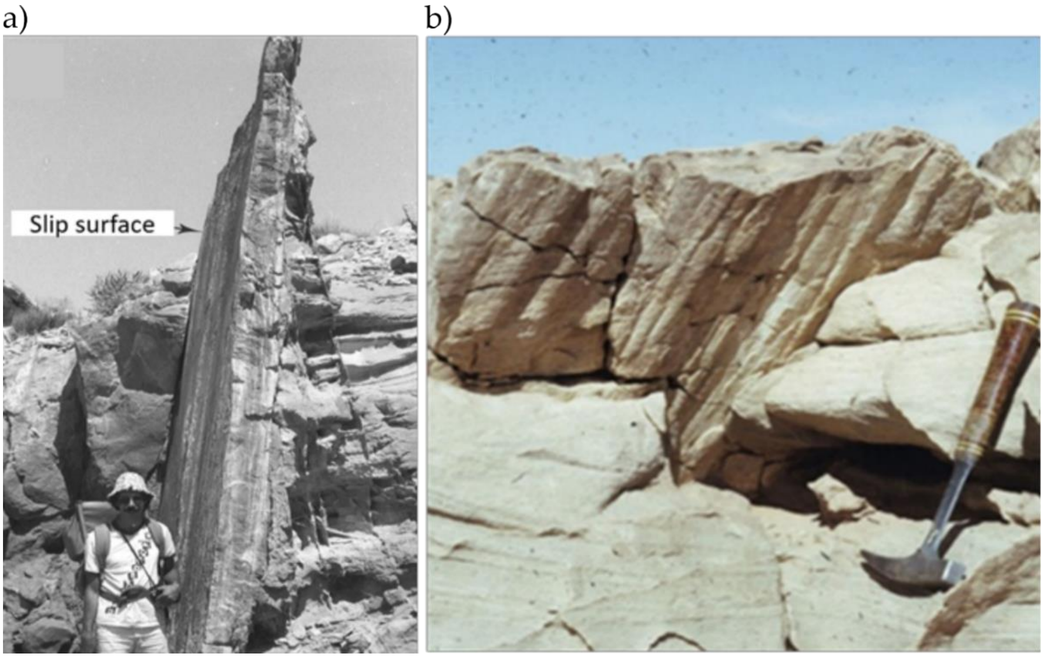

Figure 10 - a) Fault zone with a well-developed planar slip surface offsetting flat beds by about 8 m. b) Grooves and striations on a polished slip surface. Entrada Sandstone near Goblin Valley, Utah, USA. From Aydin and Johnson (1978).

Splay fractures (Figure 9b) are also known as tail cracks, wing cracks and horsetail fractures. These features can be used to identify faults and the sense of shear across them. Splay fractures are oriented at an angle to faults. This angle is usually dihedral and is called splay angle or kink angle. Box 1↴ provides additional information about splay fractures associated with strike-slip faults and their properties. Interestingly, contrary to a wide-spread misconception of shear fractures as conduits for flow, it is primarily the splay fractures and related structures known as pull-aparts that aid fluid flow rather than the shear fractures/faults or slip surfaces themselves.

Generally, offsets of horizons such as the gray-shaded units in Figure 9a do not reveal the mechanism of faulting and the exact orientation of kinematics vectors (fault slip direction). This information can be obtained by investigating nearly planar fault surfaces with a polished appearance (Figure 10a) and/or with striations and grooves (Figure 10b). Of course, three-dimensional (3D) exposures of single faults and offset horizons (Figure 10a) allow the precise assessment of fault slip direction and magnitude. The small faults shown in Figure 9a have no free ends, rather they abut against interfaces and do not stop in the middle of a bed. This lack of free ends is relevant to fluid flow in two ways.

1. The vertical hydraulic connectivity provided by faults that lack free ends is limited to the beds they crosscut. In the case of Figure 9a, it means that the faults do not create direct hydraulic communication between the yellow bed where they stop and the bed directly above or below their tip location. Specifically, in Figure 9a:

- the near-vertical fault in the center of the diagram provides communication between all three yellow layers;
- the lower left fault provides communication between the lower two yellow layers; and,
- the upper right fault provides communication between the upper two yellow layers.

2. The efficiency of fluid flow in settings where faults lack free ends depends not only on the permeability of the faults themselves but also on the geometry (continuity) and permeability of the interbed contacts (i.e., the horizontal lines between the yellow and grey beds in Figure 9a). For example, if the grey beds of Figure 9a are permeable, then flow in the near-vertical faults may enter those beds and continue horizontally along and/or vertically through the beds to eventually seep into:

- the adjacent yellow beds; and/or,
- into other faults which will in turn provide new pathways.

5 Deformation Bands

This section briefly introduces structures collectively called deformation bands, which represent localized deformations grouped into narrow bands (Rudnicki and Rice, 1975; Aydin et al., 2006). The image in Figure 11a shows one compaction band (the pen is for scale) and two shear bands, which can be identified by the offsets of the older bands, in the Aztec Sandstone at Valley of Fire State Park, Nevada, USA.

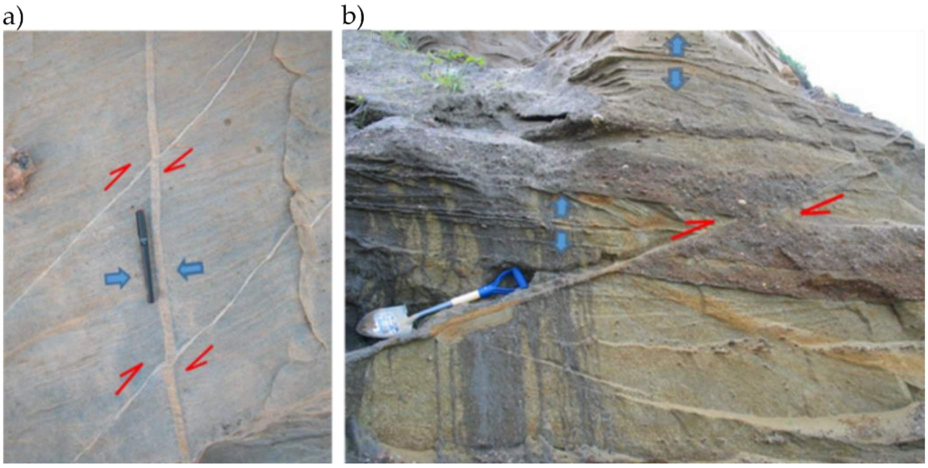

Figure 11 - a) A compaction band (marked by a pen and blue arrows) that is cut and offset by two shear bands (marked by red half arrows), showing that the compaction band is older. Aztec Sandstone, Valley of Fire State Park. b) A low-angle thrust fault (marked by shovel) in poorly consolidated terrace deposits near Arcata, northern California, USA. Based on the sense of fault motion, subhorizontal bands must have been dilated. Additional information about structures known as dilation bands is provided by du Bernard and others (2002).

Often, different types of deformation bands crosscut the same rock volumes (Figure 11a). In Figure 11a, converging blue arrows represent the constriction direction which is normal to the compaction band, whereas red half arrows mark upward-to-left direction of shearing across two subparallel shear bands. The compaction band is older than the shear bands. Generally, compaction bands are thicker than shear bands by as much as an order of magnitude. The annotated image in Figure 11b shows a shear band in the diagonal orientation with the thrust motion marked by red half arrows in young, poorly-consolidated, terrace deposits in Northern California, USA (Cashman and Cashman, 2000). The bands in the subhorizontal orientation are dilation bands (du Bernard et al., 2002) with the opening direction marked by diverging solid blue full arrows as inferred from the sense of shearing on the shear band. Mollema and Antonellini (1996) present similar configurations of compaction bands.

The striking differences in the geometry and orientation of the bands reported in Figure 11a and Figure 11b are strictly related to their formation mechanics. The two factors prominent in the formation of deformation bands are stress state (Figure 12a) and material properties (Figure 12b). The semi-parabolic curve in the *p*-*q* (mean stress *p* vs. shear stress *q*) diagram of Figure 12a represents the failure envelope limiting the admissible stress states and controlling the nature (arrow labeled "m") and orientation (labeled "n") of the failure structure. The notion is that the loading paths and incremental plastic deformation control the geometry and nature of the failure structures. Material properties of the granular medium (porosity, grain size, and degree of cementation and strength of grain contacts) control the micromechanics of deformation (Figure 12b) involving pore enlargement (dilation) or pore collapse (compaction), grain-to-grain sliding without appreciable volume change (isochoric shear) and grain fracture (cataclastic deformation with compaction). More information on this topic is provided by Aydin and others (2006) and Schultz (2019).

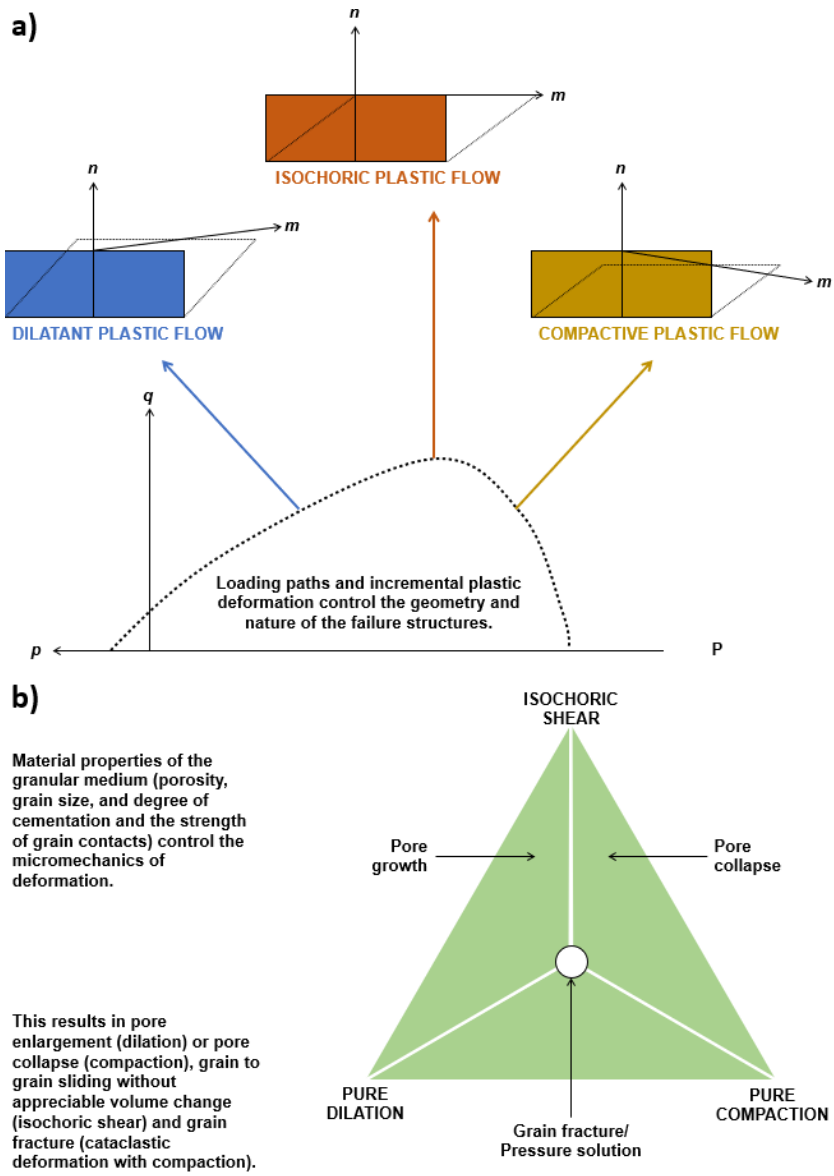

Figure 12 - a) A diagram, commonly referred to as *p-q* diagram, showing the failure envelope and range of mechanical behaviors as a function of mean stress *p* and shear stress *q*. b) A ternary diagram showing domains of micro-mechanisms with isochoric shear, dilation and compaction (Dippenaar, 2022, based on Aydin et al., 2006).

6 Fracture Zones

Zones of fracture types listed in Figure 2 are detailed below, beginning with joint zones (Figure 13) and continuing with deformation band zones and fault zones.

a) b)

Figure 13 - Joint zones or clusters at Entrada Sandstone, Arches National Park, Utah, USA. a) A joint zone of about 60 to 80 cm in width including several single joints with spacing considerably narrower than that between the zone and the nearest joints on either side of the zone. b) Localization of joints adjacent to high-angle small faults. From Cruikshank and Aydin (1995).

6.1 Joint Zones

Joint zones, also known as joint clusters, fracture corridors (or swarms), refer to more than two (commonly many) individual joints localized in a narrow zone, as shown in Figure 13. These features are significant conduits for fluid flow. Joint zone widths measured in the field vary from centimeters to tens of meters. Figure 13a shows a joint zone about 60 to 80 cm in width that is composed of several subparallel joints in the Entrada Sandstone at Arches National Park, Utah, USA. The photograph in Figure 13b shows a joint zone that is localized in a specific horizon and associated with several sheared vertical joints behind the person placed for scale (Cruikshank and Aydin, 1995). The formation of joint zones may be controlled by the velocity of the joint growth (Olson, 2004). When this mechanism is active, clustering can occur for very high values of the subcritical index. The subcritical index relates the stress intensity factor (which predicts the stress state near the fracture tip) to the fracture propagation velocity.

Other possible fracture clustering mechanisms involve specific tensile stress patterns (in such cases tension halos develop around fractures) and mechanical interactions between fractures repeated through time (de Joussineau and Petit, 2021). These examples indicate that there are different mechanisms for joint zone formation, including shearing. Further information related to the geometrical properties of fracture corridors is provided by de Joussineau (2023).

As noted earlier, once formed, almost all joint zones represent weak zones prone to shearing, which improves the connectivity between neighboring fractures in the zone as well as between the zone and the neighboring joints or joint zones.

6.2 Compaction Band Zones

The photographs in Figure 14 show zones of compaction bands composed of subparallel, closely spaced, single compaction bands in Aztec Sandstone, Valley of Fire State Park, USA. Figure 14a shows a simple zone with a few individual bands. An image of multiple compaction band zones in Figure 14b shows a series of eye structures formed by overlapping neighboring zones with individual zigzag bands inside and outside of the relay zone which is located between and delimited by the main segments of the compaction bands.

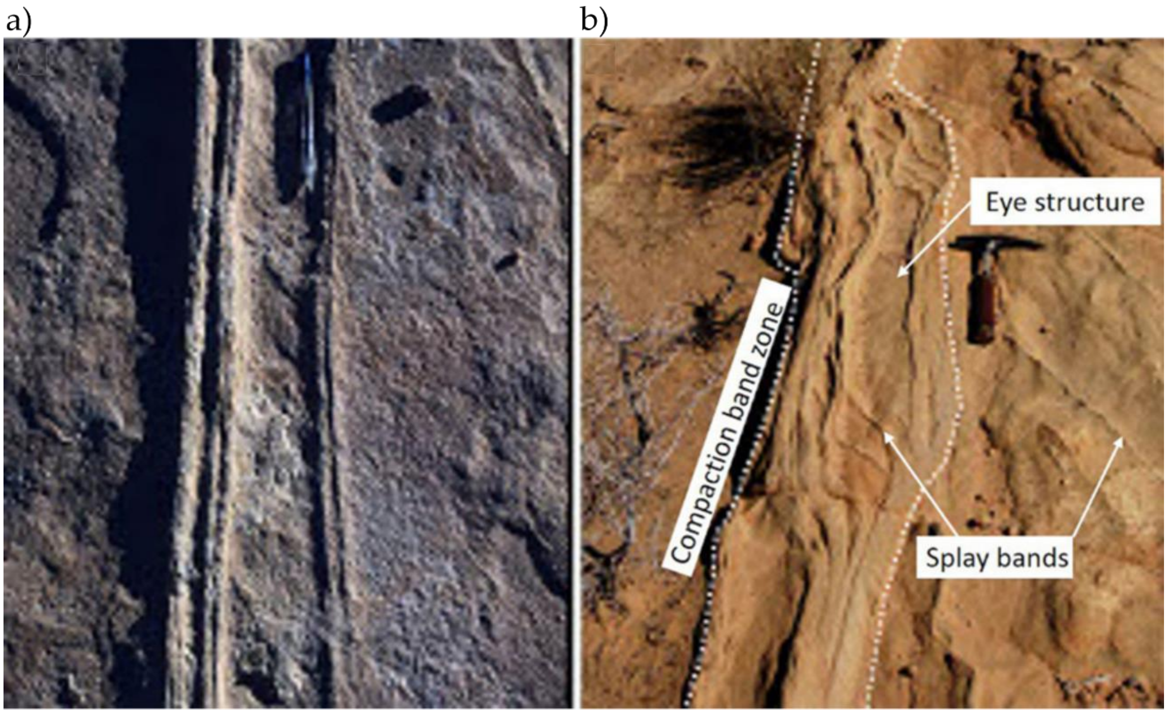

Figure 14 - Compaction band zones. a) A narrow band with a few single subparallel bands. b) A well-developed compaction band zone with overlapping bands and their splays. From Aydin and Zhong (2017).

The compaction band zones in Figure 14a and Figure 14b developed by the sequential formation of individual bands adjacent to one another, as schematically reported in the series of diagrams of Figure 15a-d. The simplest case is when adjacent bands sequentially develop parallel to one another (Figure 15a). Adjacent bands may interact with each other, partially overlapping and converging, and either forming eye structures (Figure 15b) or diverging away from the zone (Figure 15c). Figure 15d shows a more complex zone with several zigzag splays or tail bands (further details are provided by: Eichhubl et al., 2010; Liu et al., 2015).

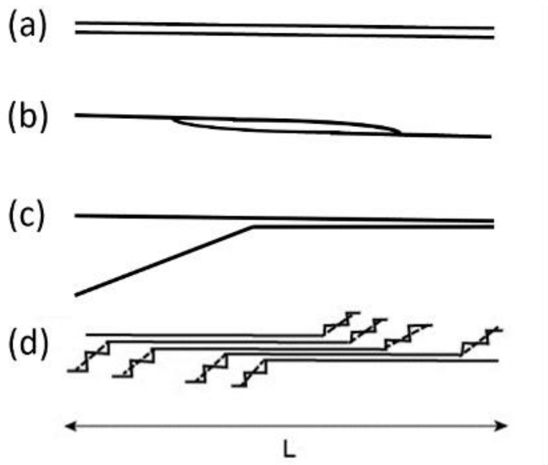

Figure 15 - Schematic diagrams showing compaction band zones: a) subparallel bands; b) converging and overlapping bands forming an eye structure; c) subparallel and diverging bands; and, d) subparallel bands with complex splays.

6.3 Shear Band Zones

The photographs in Figure 16a and Figure 16b show zones of shear deformation bands, often referred to as zones of shear bands. The slip on the small zone in Figure 16a is about 5 mm, whereas it is about 3 to 4 m across the zone in Figure 16b. The exposed portion of the scale in Figure 16b is about 75 cm. Similar to the growth of compaction band zones illustrated earlier, shear band zones also grow by sequential addition of individual shear bands, one adjacent to the other.

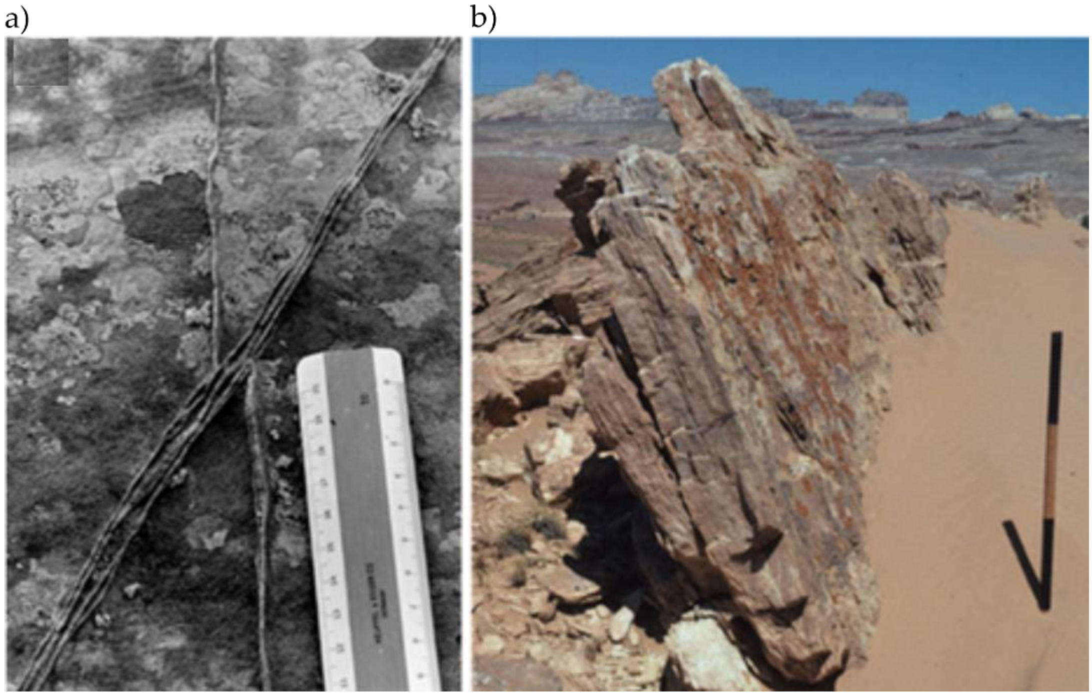

Figure 16 - Shear band zones. a) A small zone with a few shear bands offsetting an older band for about 0.5 cm. b) A larger shear band zone with a normal sense of offset of about 3.5 m. The exposed portion of the scale in Figure 16b is about 75 cm. From Aydin and Johnson (1978).

The plot in Figure 17 shows how the permeability of shear band zones (simply referred to as deformation bands) may depend on the number of bands as well as on the permeability of individual bands (Shipton et al., 2002). Overall, the value of permeability across shear band zones decreases as the number of bands increases.

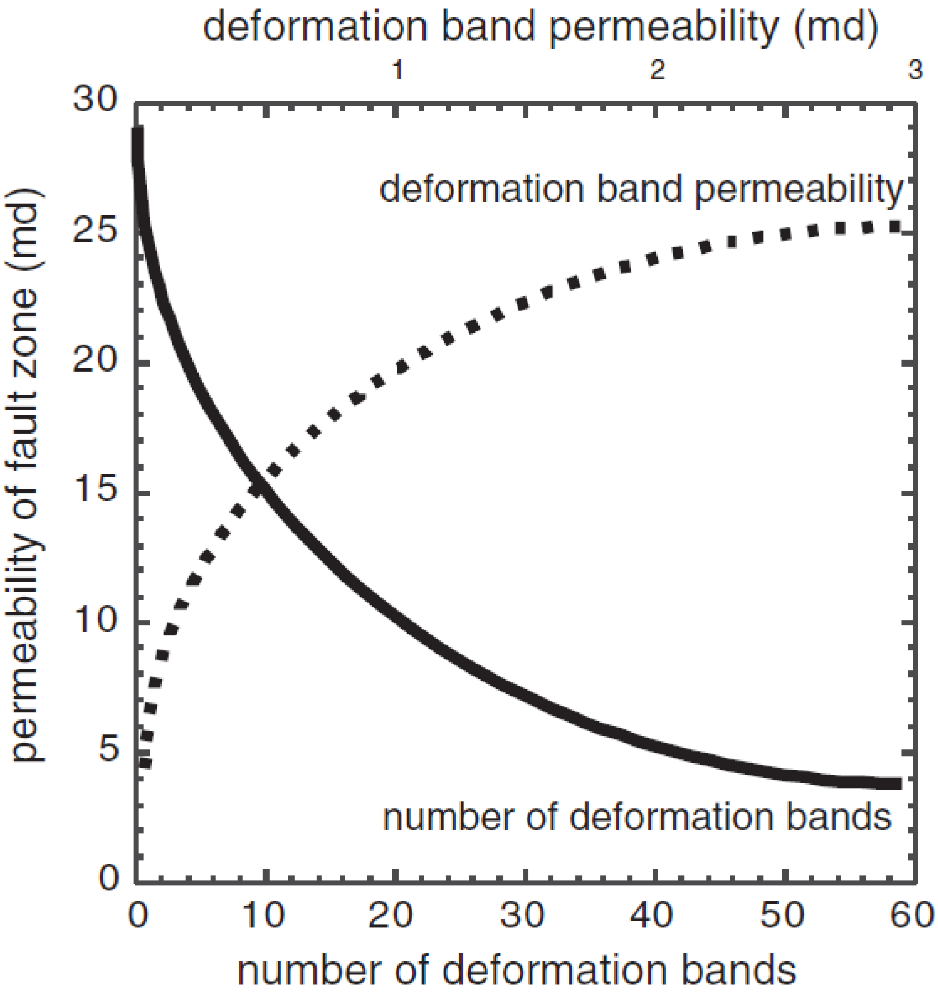

Figure 17 - A plot showing how the number of bands and band permeability (in millidarcy, mD) may affect the permeability of shear band zones. From Shipton and others (2002).

More realistic values of a deformation band zone permeability can be estimated by using actual single band permeability. The compilation of data shown in Table 1 includes porosity and permeability of compaction bands in various orientations to the cross-bedding and shear bands. Permeability was obtained by use of a field or lab mini-permeameter.

Table 1 – Permeability (in millidarcy) and porosity of deformation bands and their host rocks. Compiled by Deng and others (2012) from the sources listed in the first column.

Previous Studies	Permeability of Host Rocks [mD]	Permeability of Compaction Bands [mD]	Porosity of Host Rocks [percent]	Porosity of Compaction Bands [percent]
Antonellini& Aydin, 1994	1,000 - 5,000	10 - 500	~18	~6 - 12
Floding et al., 2005	123 - 5,991	N/A	16.6 - 24.4	N/A
Keehm et al., 2006	200 - 3,500	1 - 20	20 - 27	9 - 12
Aydin & Ahmadov, 2009	860 (average)	146 (average)	~24	~11
Lenoir et al., 2013	1,000	0.0006	~21	~14.5
Sun et al., 2011	1,300 (average)	210 (average)	~20	~14
Fossen et al., 2011	~20 - 1,000	~0.3 - 200	~26 - 32	~0 - 100 porosity reduction relative to host rock
Deng et al., 2015b: high-angle sets	~140 - 487	~0.27 - 0.87	~21 - 32	~11 - 18
Deng et al., 2015b: bed-parallel sets	~784 - 2,313	~3.68 - 755	~21 - 32	~13 - 24
Torabi et al., 2015	N/A	N/A	17 - 30	8.8 - 19.7

6.4 Fault Zones

The schematic diagram in Figure 18 represents the major components of a fault zone: a fault core with one or many slip surfaces, and damage zones commonly flanking the fault core on both sides. The fault core contains deformed rock accumulated during the fault growth. Both fault core and damage zones evolve during the history of faulting through various deformation mechanisms (Aydin and Berryman, 2010), and therefore show a wide range of variations. A short introduction to the case study of fault zones in Aztec Sandstone at the Valley of Fire State Park, Nevada, USA, is presented in this section.

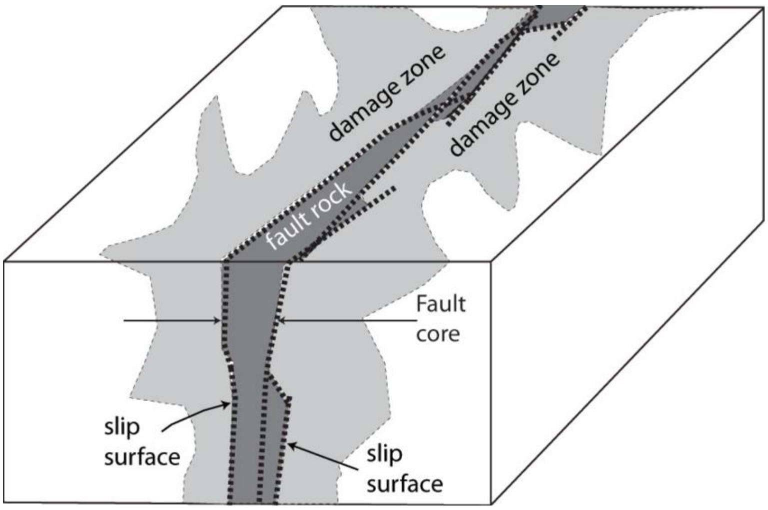

Figure 18 - Idealized diagram showing fault zone elements, including the fault core, which includes fault rock and several slip surfaces, and the surrounding damage zone. From Aydin and Berryman (2010).

Figure 19 shows a photograph of a fault zone in the Aztec Sandstone with its core and damage zone identified. This fault zone has a 14 m left-lateral slip based on matching dune units on two sides of the fault.

Figure 19 - Photograph showing a portion of a fault zone with a 14 m left-lateral slip in the Aztec Sandstone at Valley of Fire State Park, Nevada, USA. The fault core and associated damage zone on both sides are visible. From left to right, Ghislain de Joussineau, Joseph Gonzales and Ramil Ahmadov provide a reference for scale. From Aydin and Zhong (2017).

Figure 20 is a close-up of a part of this zone, not far from the top side of the area covered by the larger view in Figure 19. Arrows mark several slip surfaces in the detailed photograph. It is possible to identify reddish infills along these surfaces. These are called “slip bands” (Ahmadov, 2006; Ahmadov et al., 2007). Slip bands along the core marked by arrows are continuous within the photos, but other bands that are discontinuous are generally diagonal to the overall direction of the core. Many of these are earlier slip bands that rotated during the evolution of the fault zone, and eventually became inactive during fault growth. Some properties of slip bands including their composition and permeability are reported in Box 2↴.

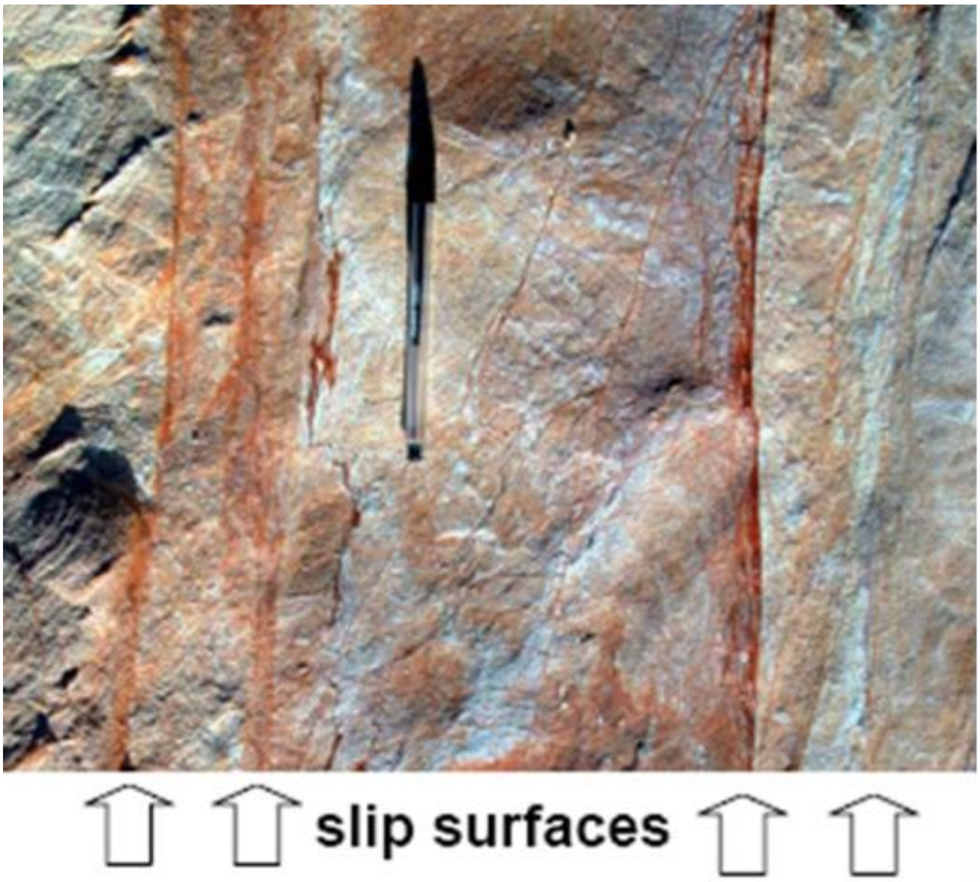

Figure 20 - Close-up photograph of the fault in Figure 19. Relatively continuous slip surfaces with reddish-stained slip bands in the fault core are marked with arrows below the photograph. Modified from Ahmadov and others (2007).

The upscaled (or effective) permeability of a small-scale fault zone with 14 m of left-lateral slip is plotted in Figure 21. The overall computed permeability normal to the fault zone (k_1 or k_x) is 8 mD and 44 mD for each 5 × 5 m block, respectively, whereas the overall computed permeability parallel to the fault zone (k_2 or k_y) is 1,320 mD and 1,480 mD for each block, respectively. The latter values are smaller and greater, respectively than the average host rock permeability of about 200 mD (Jourde et al., 2002). This is due to low permeability across the crushed fault core and high permeability along the damage zone. Additional examples of fluid flow modeling in fractured rocks are provided by Manzocchi and others (1999), Flodin and others (2004), Karimi-Fard and others (2004) and Spence and others (2014).

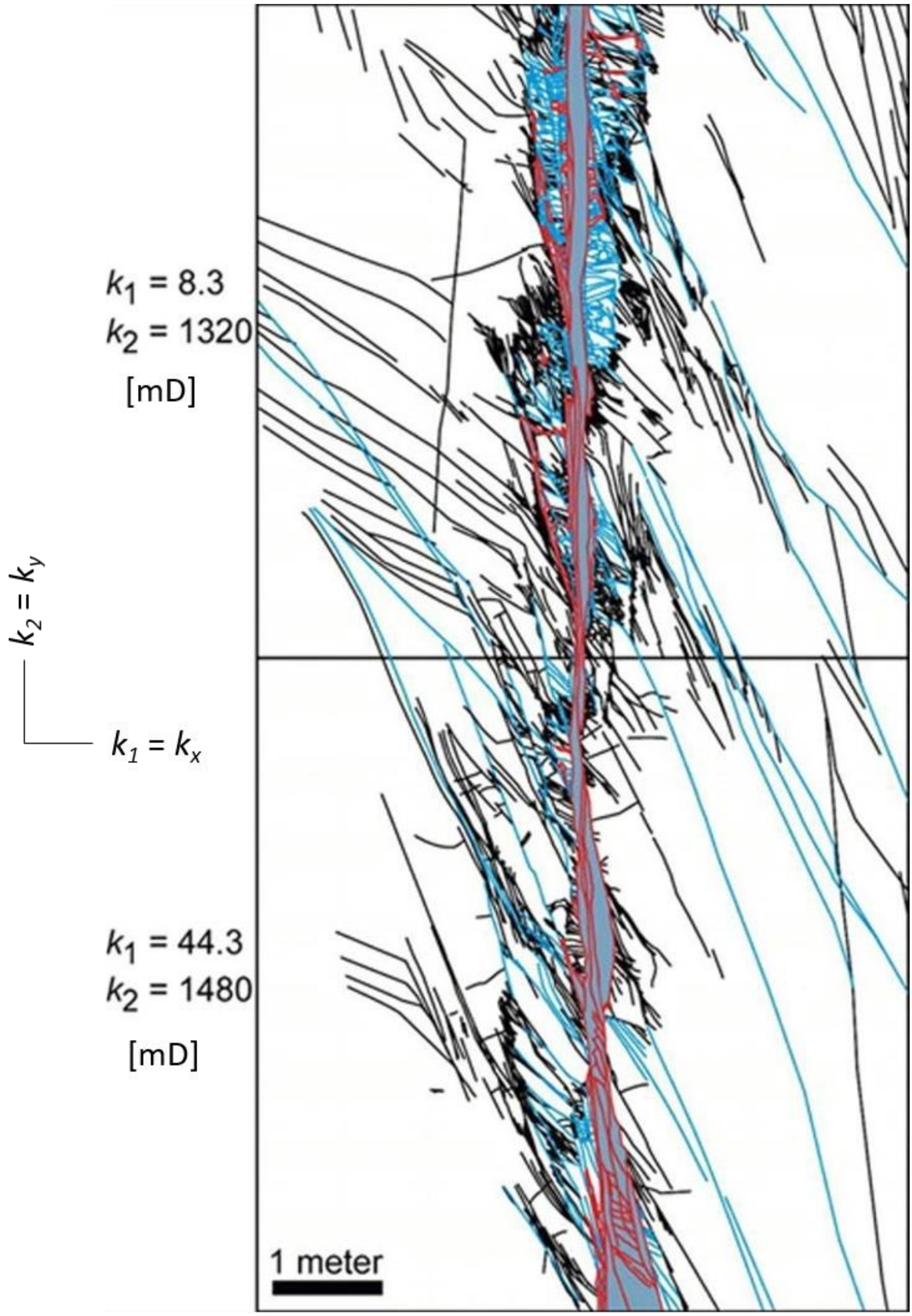

Figure 21 - Upscaled (i.e., effective permeability, *k*) of two adjacent 5 × 5 blocks along the fault shown in Figure 19 and Figure 20. The bird's-eye view of the fault map shown here is from Myers (1997) and the upscaling model is from Jourde and others (2002).

7 Fracture Sets

A series of subparallel fractures of the same type is classified as a fracture set. This section describes joint sets.

7.1 Single Joint Sets

The aerial photograph in Figure 22 shows a set of joints in the Moab member of the Entrada Sandstone at Arches National Park, Utah, USA. There, the dominant joint set is parallel to the axis of the Salt Valley Anticline. The critical properties of joint sets such as those reported in Figure 22 are their spacing and the continuity of individual elements in the array. The spacing of joints in siliciclastic rocks depends on the thickness of units in which they occur as well as the loading. The simplest common case is the proportionality between bedding thickness and joint spacing. However, the magnitude of strain in the direction perpendicular to the set is also an important factor.

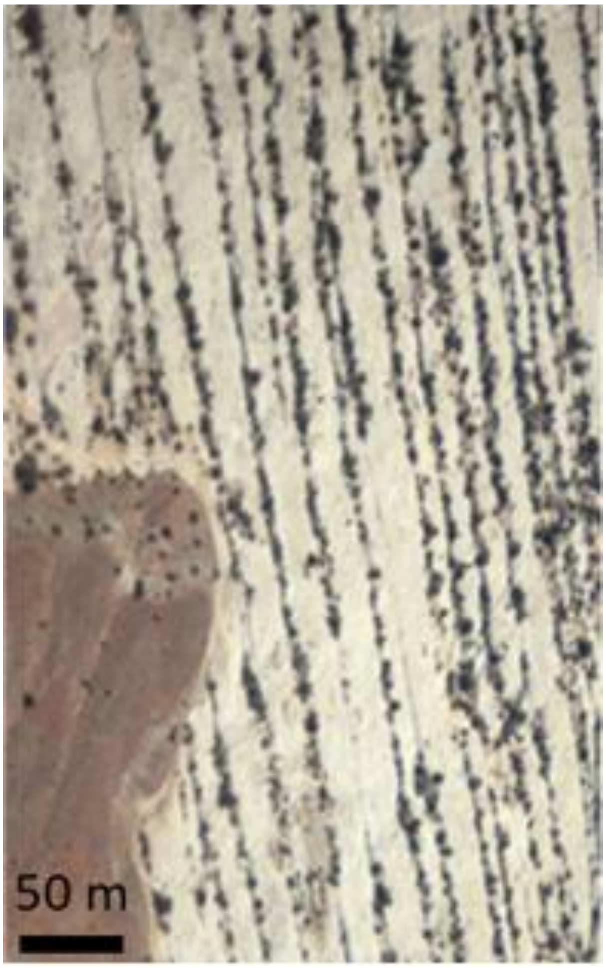

Figure 22 - Bird's eye view of a systematic joint set and other associated fractures in the Moab member of Entrada Sandstone exposed on the northern limb of Salt Valley Anticline, Arches National Park, Utah, USA. The width of the photograph, taken from an airplane, is about 300 m.

There are two main concepts related to the growth of joint sets. The first is the notion of fracture saturation, which corresponds to a critical level of joint production beyond which the number of joints does not change appreciably. In this case, any amount of additional extension is accommodated by increasing joint apertures. In layered rocks, the joint spacing to layer thickness ratio appears to level off around unity for fairly well-developed joint systems. In such systems, the spacing of joints is controlled largely by the height of the joints, the basis of which is the stress shadow zone that forms around joints (Lachenbruch, 1961). The second important concept is the interaction between closely spaced joints (Pollard and Aydin, 1988). A particular geometry referred to as *en échelon* (here echelon for simplicity) and relays, implies the possibility of gaps in the lateral continuity of the joints. The continuity of joints or the lack thereof is important for fluid flow. As mentioned earlier, even though the lineaments such as those in Figure 22 may appear to be continuous, a close inspection may reveal gaps along them or, in other words, space between the consecutive echelons. In general, the segmentation of joints in both lateral and vertical directions is the rule and not an exception. A wide range of observations tells us that it is very difficult for joints (or any fracture type) to propagate within a plane over a long distance. The main reasons for this are the presence of widespread material inhomogeneities in rocks and the interactions among adjacent fractures during ongoing deformation.

7.2 Multiple Joint Sets

In low-porosity sedimentary rocks, two sets of joints at right angles to each other form an orthogonal pattern. The simplest cases of these have grid and ladder-like patterns, as idealized in the sketches of Figure 23. These patterns are inherited from changes in the stress regime through time, involving a switch between the intermediate and minimum stresses σ_3 and σ_2, respectively. This switch may be related to changes in the local regional stress field, or to stress release on newly formed systematic fractures.

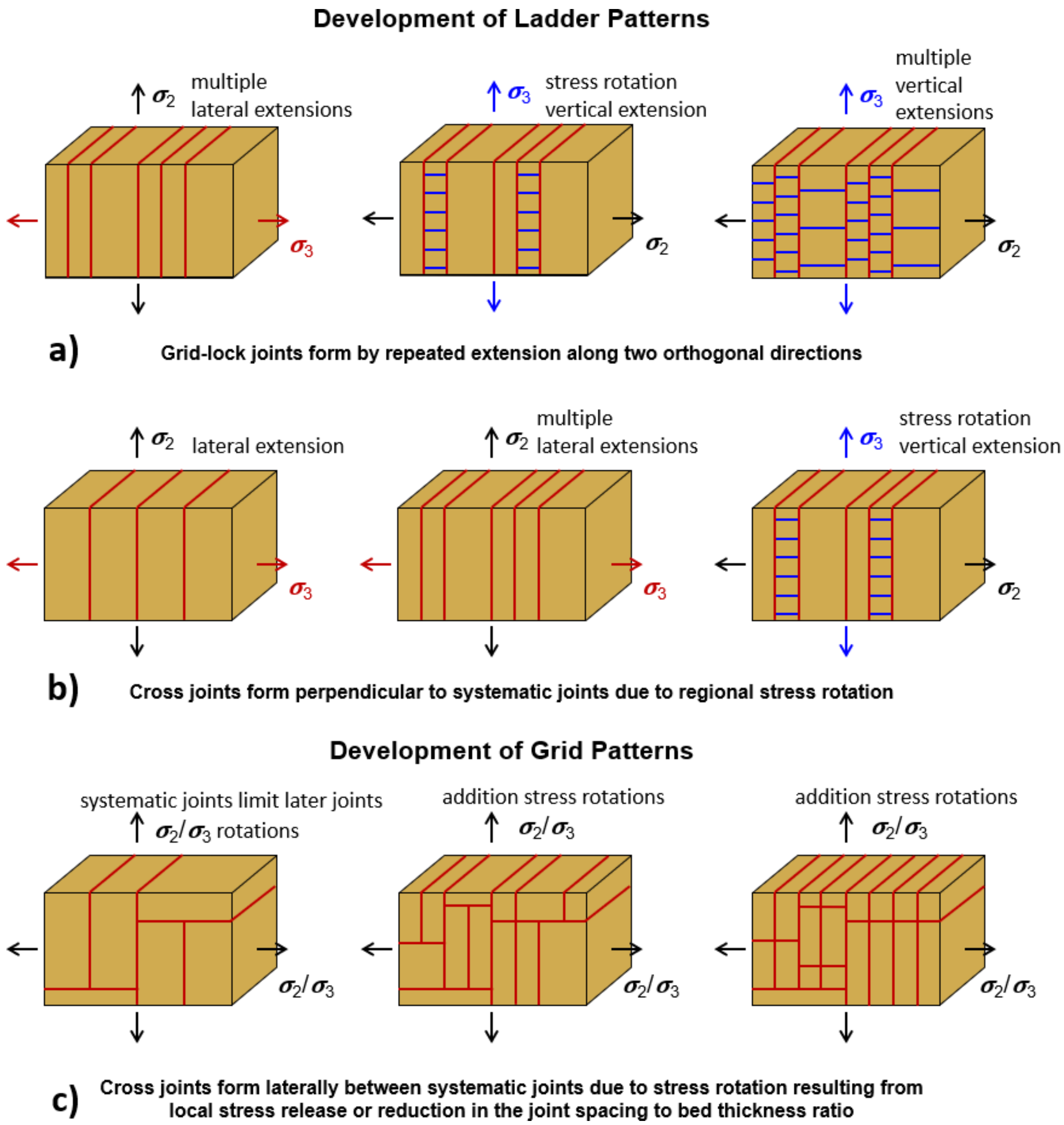

Figure 23 - Ladder and grid patterns of orthogonal joints (Dippenaar, 2022).

Figure 24a shows an orthogonal joint pattern in a siltstone/mudstone outcrop. Figure 24b shows an orthogonal joint pattern produced in a glass plate by sequential bending in the laboratory. Some members of each set may initiate from, and terminate at, members of the other set as marked by yellow circles. The critical factor is their abutting geometry indicating their temporal relationship (i.e., the order of fracture genesis). The fluid flow behavior may be affected by the abutting styles of the joints. If all the joints are open, flow paths along second-generation joints have a higher tortuosity compared with flow paths along first-generation joints (Figure 23). This imparts a hydraulic conductivity anisotropy to the fractured rock.

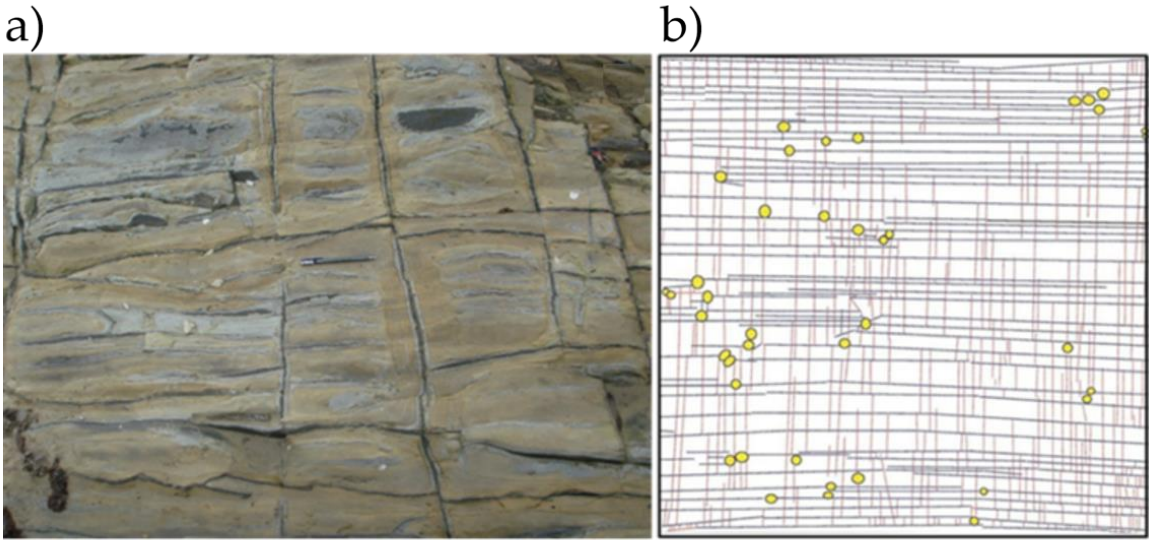

Figure 24 - a) Photograph showing orthogonal joints in siltstone/mudstone exposure at the Pacific Coast, north of Santa Cruz, California, USA. b) Orthogonal joint sets in a glass plate produced in a laboratory by sequential bending. Yellow circles mark the initiation points of individual joints. Photograph courtesy of Haiqing Wu of Stanford University in 1999.

8 Deformation Band Sets

Following the kinematic classification of single deformation bands, this section discusses sets of compaction bands. Sets of shear bands are discussed in Section 10 and sets of dilation bands, which are rather rare and difficult to identify both in the field as well as in cores, are not discussed.

The map in Figure 25 shows multiple sets of compaction bands first recognized by Hill (1989) in the Cottonwood Wash area of the Valley of Fire State Park, Nevada. It includes three sets marked as 1, 2 and 3 on the map. A fourth set along the low-angle cross-beds is not visible on the map. Aydin and Ahmadov (2009) subsequently documented these features and introduced the concept of bed-parallel compaction bands. Two of the sets, labeled 1 and 2, are broadly spaced and are at right angles to each other. The third set, labeled 3 by Hill (1989), is confined between sets 1 and 2 and is characterized by narrower spacings, shorter lengths and a zigzag geometry. This set is analogous to the anti-cracks of Mollema and Antonellini (1996) and shear-enhanced compaction bands of Eichhubl and others (2010). Compaction bands form in porous rocks normal to the maximum compressional stress direction, and their hydraulic behavior is like that of shear deformation bands. The maximum permeability reduction is in the direction normal to the compaction band. These structures, therefore, introduce a strong anisotropy of hydraulic conductivity in the rock masses and should be considered when assessing groundwater flow pathways.

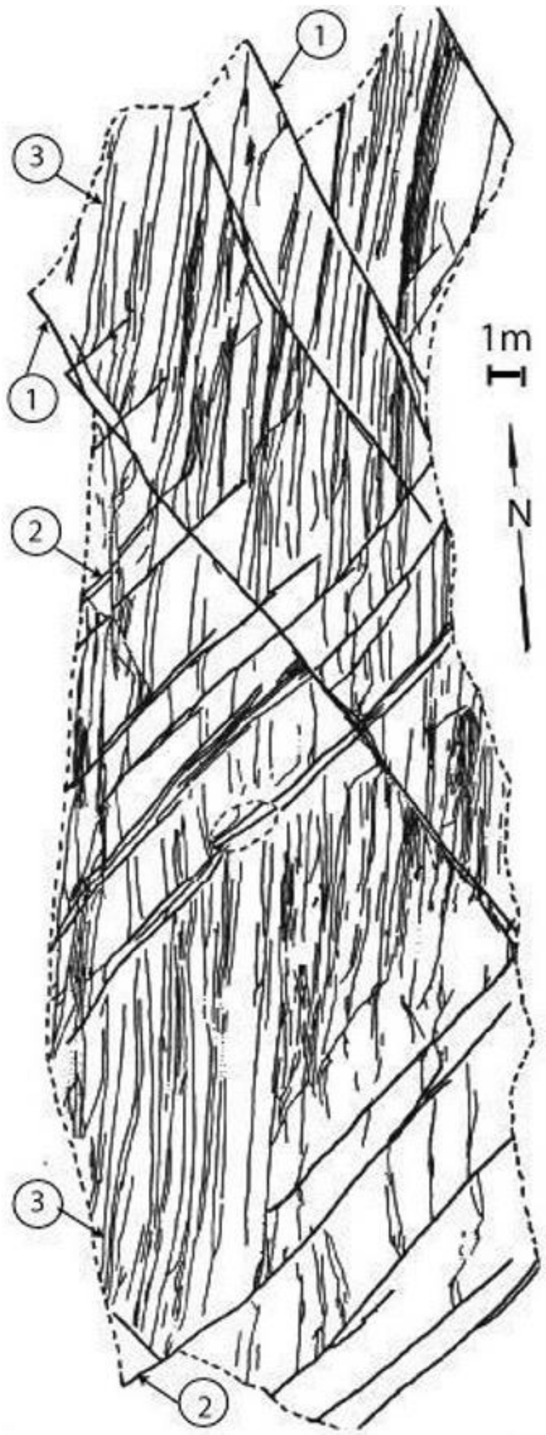

Figure 25 - Multiple sets of compaction bands in Aztec Sandstone cropping out at Cottonwood Wash in Valley of Fire State Park, Nevada, USA, were originally mapped and described by Hill (1989). Two of the sets, labeled 1 and 2, are broadly spaced and at right angles to each other. The third set, labeled 3, is confined between sets 1 and 2 and has narrower spacings and shorter lengths. Later, this set was interpreted as a shear-enhanced compaction structure by Eichhubl and others (2010).

Figure 26 illustrates the relationship between the presence and orientation of compaction bands and cross-beds in the Aztec Sandstone. The outcrop reported in this figure is not far from the locations where Hill (1989) and Aydin and Ahmadov (2009) mapped high-angle-to-bedding and bed-parallel compaction bands. The annotated photograph shows two adjacent dune packages with cross-beds at different orientations and associated compaction bands (Figure 26). One domain of high-angle-to-cross-beds compaction bands occurs at the upper dune, and the other domain of compaction bands occurs parallel to the cross-bed at the lower dune. It then follows that as the cross-bed orientations vary from one dune package to the next, so do the compaction band orientations as shown in the schematic block diagram in Figure 27. This interdependence is attributed to the anisotropy introduced by the depositional structures, primarily cross-beds (Deng and Aydin, 2012; Deng et al., 2015a).

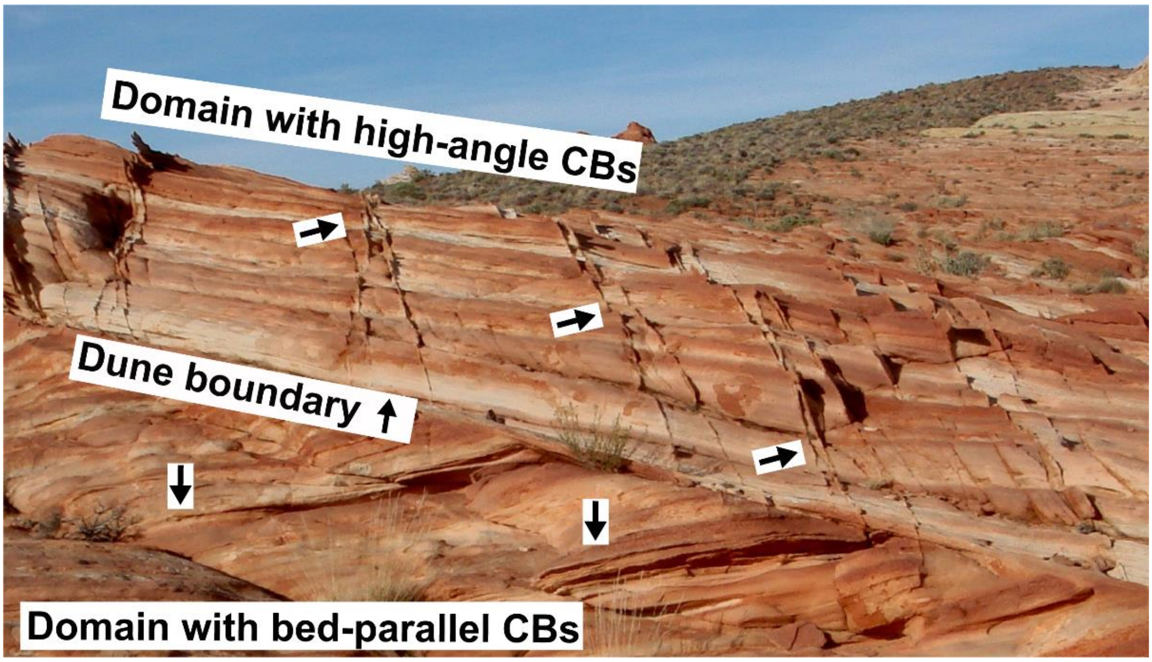

Figure 26 - Distribution of compaction bands (CBs) in adjacent dunes with different cross-bed architectures in the Valley of Fire State Park, Nevada, USA. One set of high-angle-to-bedding compaction bands is pointed out by horizontal arrows in the upper dune with a distinct cross-bed orientation (light and red diagenetic colors of beds). Another set of compaction bands occurs parallel to cross-beds in the lower dune with noticeably different cross-beds. From Deng and Aydin (2012).

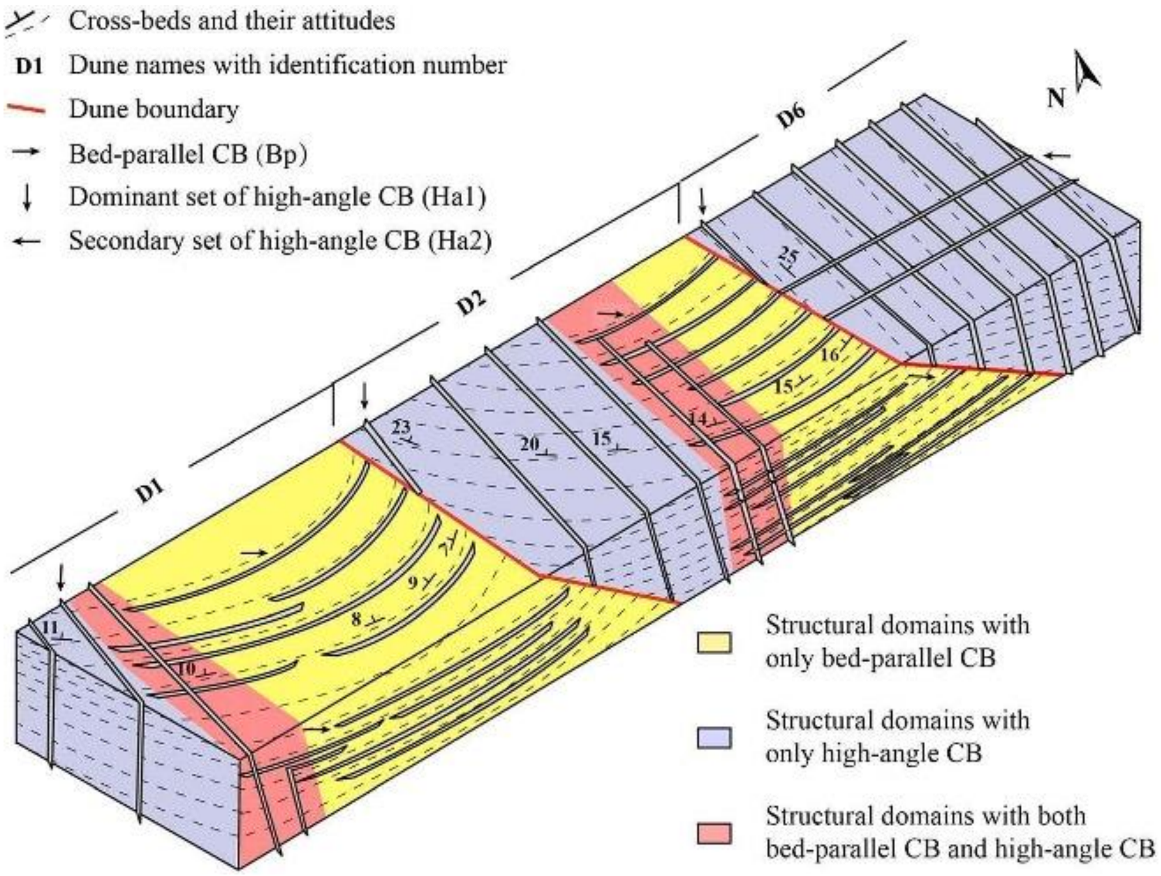

Figure 27 - Schematic diagram illustrating compaction band (CB- bed-parallel Bp and high-angle Ha) patterns adopted from dunes (numbered D1, D2 and D6) and cross-beds therein. From Deng and Aydin (2012) and Deng and others (2017).

The schematic diagram in Figure 27 depicts the variation of compaction band orientation controlled by a geometry of multiple dune packages to form the following sets: high-angle set, bed-parallel set, two intersecting high-angle sets, and both high-angle and bed-parallel sets. These are idealized from an exposed section in the field that passes through dunes D1, D2 and D6 as labeled by Deng and Aydin (2012).

9 Compaction Bands and Permeability Upscaling

The compaction bands mapped in the field can be integrated into a model that may be used to create the permeability distribution required by a flow simulator. Deng and others (2017) presented a case that starts from an outcrop map of compaction bands in aeolian sandstone and in-situ measurements, then upscales the permeability to the aquifer or reservoir scale.

Figure 28a and Figure 28b show idealized block diagrams of 40 m × 40 m × 5 m with multiple compaction band domains and the corresponding model configuration, respectively. The domains of compaction bands based on field data are color-coded in Figure 28a, and idealized compaction bands are represented in Figure 28b.

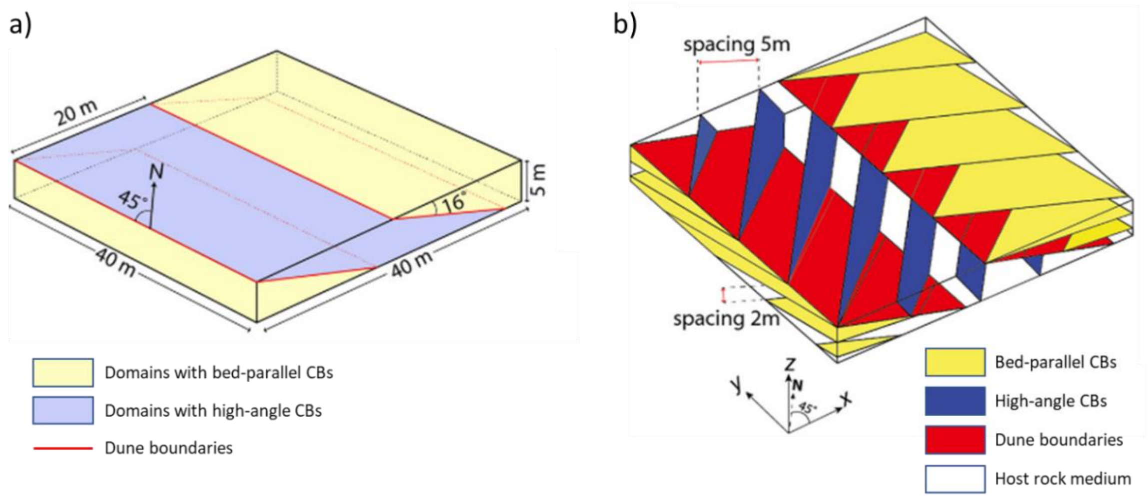

Figure 28 – a) Domains of compaction band patterns based on field observations. b) The average spacing of high-angle compaction bands and low-angle bed-parallel compaction bands are about 5 m and 2 m, respectively. The Cartesian coordinates provide orientation. From Deng and others (2017).

Deng and others (2017) used the permeability values and the spatial properties of deformation bands measured in outcrops of dunes of aeolian sandstone that are provided in the inset of Figure 29 to calculate and plot the 3D upscaled permeability shown in Figure 29. For this computation, they employed a discrete-feature model developed by Karimi-Fard and others (2004) and a permeability upscaling procedure for fractured rock developed by Wen and others (2003) and Flodin and others (2004).

Inset

Parameters	Case 1
Matrix permeability, k_m (mD)	500
Matrix porosity	0.25
High-angle CB permeability (mD)	5
High-angle CB porosity	0.17
High-angle CB thickness (cm)	20
High-angle CB spacing (cm)	500
Bed-parallel CB permeability (mD)	5
Bed-parallel CB porosity	0.17
Bed-parallel CB thickness (cm)	15
Bed-parallel CB spacing (cm)	200

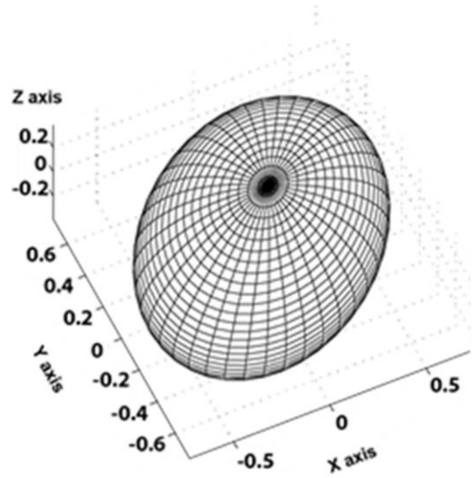

Figure 29 - Table of permeability values (inset) used for flow simulation and calculated upscaled permeability for one case labeled Case 1. From Deng and others (2017).

Deng and others (2017) ran several upscaling cases with varying configurations (patterns) of deformation bands and varying petrophysical (porosity, permeability) and thickness properties. The model presented in Figure 29 is their base case model. Their results revealed the effect of the characteristic configuration of compaction bands on fluid flow when they calculated flow rates using the upscaled permeability components in the *x* direction (normal to the dune trend), *y* direction (parallel to the dune trend) and *z* direction (vertical direction) for several cases.

The results suggest that the upscaled permeability of the compartmentalized compaction band arrays is significantly influenced by the permeability, orientations and distribution of compaction band sets. For example, the representative configuration shown in Figure 28 includes a combination of both high-angle domain bands and bed-parallel domain bands, consequently, the upscaled permeability normal to the dune trend (*k*x*) is controlled primarily by the high-angle compaction bands because the flow in this direction crosses the high-angle compaction band domain. The orientation of the major permeability component (*k*max*) remains essentially unaffected by the change in compaction band permeability because the preferred flow path crosses the minimum number of compaction bands. However, the orientation of the minimum permeability component (*k*min*) changes significantly. These results suggest that the interplay between the spatial distributions of compaction band sets and their permeability exerts a significant influence on the orientation of the minimum permeability component (*k*min*).

10 Shear Band Sets and Their Conjugate Patterns

The map in Figure 30 shows the distribution and pattern of shear bands in the Entrada Sandstone that is exposed on the southwestern flank of Salt Valley Anticline in the Garden area at Arches National Park, Utah, USA (Cruikshank et al., 1991; Zhao and Johnson, 1992). This is a classic conjugate strike-slip fault pattern also described in sandstones from other regions; see for example Davis (1999) and Roznovsky and Aydin (2001). The inset is a photograph of a simple outcrop-scale conjugate fault pattern from Aydin and others (2006). The angle between the conjugate sets varies, as analyzed by Olsson and others (2004) and Haimson and Rudnicki (2010); the latter attribute the variation to the intermediate principal stress. This is a good example of how shear deformation bands can compartmentalize the top high-porosity section of the Entrada Sandstone. In this type of setting (i.e., shear deformation bands with small strike-slip offset), hydraulic conductivity is high in the vertical direction, whereas it is low in the horizontal direction. In the case shown in Figure 30, the maximum hydraulic conductivity is in the vertical direction, the minimum horizontal hydraulic conductivity is in the NW-SE direction (perpendicular to the densest set of bands) and the maximum horizontal hydraulic conductivity is in the NE-SW direction. Knowledge of the type of structures in a porous aquifer greatly helps in characterizing its anisotropic hydraulic conductivity.

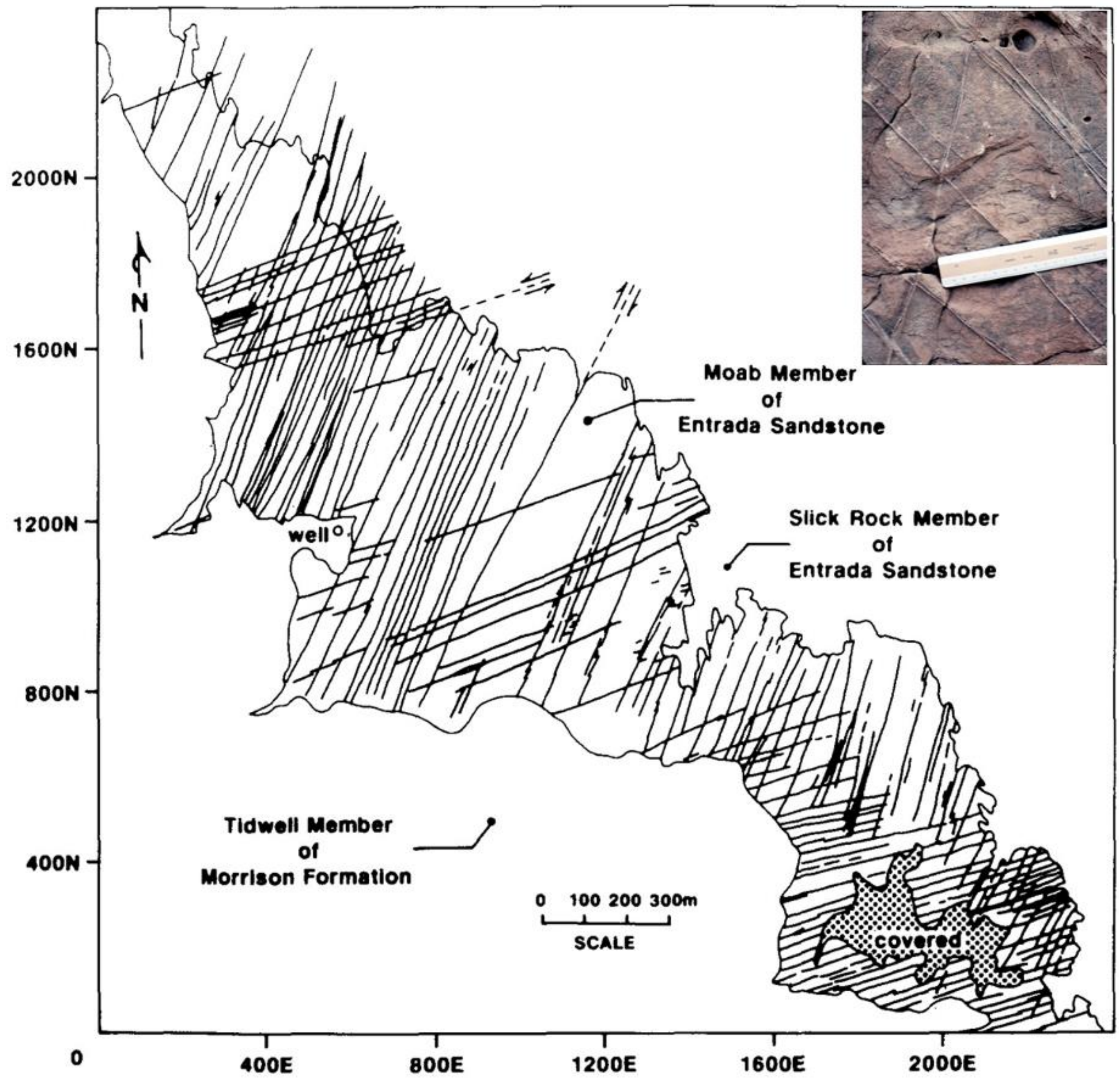

Figure 30 - Shear bands pattern in Mesozoic sandstones, primarily Entrada Sandstone in the Garden area of Arches National Park, Utah, USA. This pattern is known as "conjugate." From Cruikshank and others (1991) and Zhao and Johnson (1992).

11 Multiple Fault Sets

First, a fracture of any type rarely occurs alone. Structures such as fracture sets and multiple fault sets are part of an ontology that provides information for understanding complex systems and facilitates building the historical progressive evolution of systems. Second, fault patterns that look similar to a casual observer may be formed by quite different mechanisms. As an example, the map in Figure 31 shows a complex fault system primarily in the Aztec Sandstone in the Valley of Fire State Park, Nevada, USA. This pattern is similar to the conjugate shear bands pattern in Figure 30, but it developed through a completely different mechanism, which is sequential shearing of initial joints and the resulting splays (Myers and Aydin, 2004; Flodin and Aydin, 2004; de Joussineau and Aydin, 2007a).

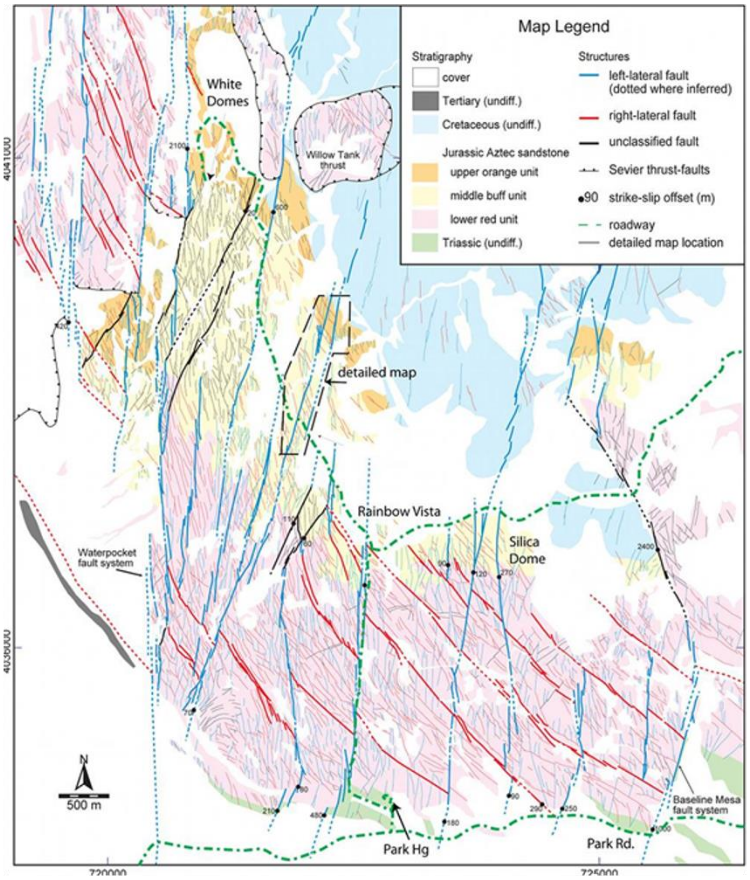

Figure 31 - Map showing a well-organized fault system primarily in the Aztec Sandstone that covers much of Valley of Fire State Park, Nevada, USA. Both the left- and right-lateral faults are distributed in a systematic pattern. This pattern is referred to as "apparent conjugate" to differentiate it from the conjugate shear band pattern shown earlier. The formation mechanism is referred to as segment and strand interactions in the next series of maps. From Flodin and Aydin (2004).

Complex fault patterns such as those in the map of Figure 31 may be analyzed by breaking them down into their components. The first step in this process is to decipher fault segments and their sequential interaction products. The maps in Figure 32 and Figure 33 are examples of the application of these concepts, the basis of which is the process of fault growth through interaction between adjacent segments and neighboring fault strands. Some parameters related to this process are defined in the diagram in Figure 34.

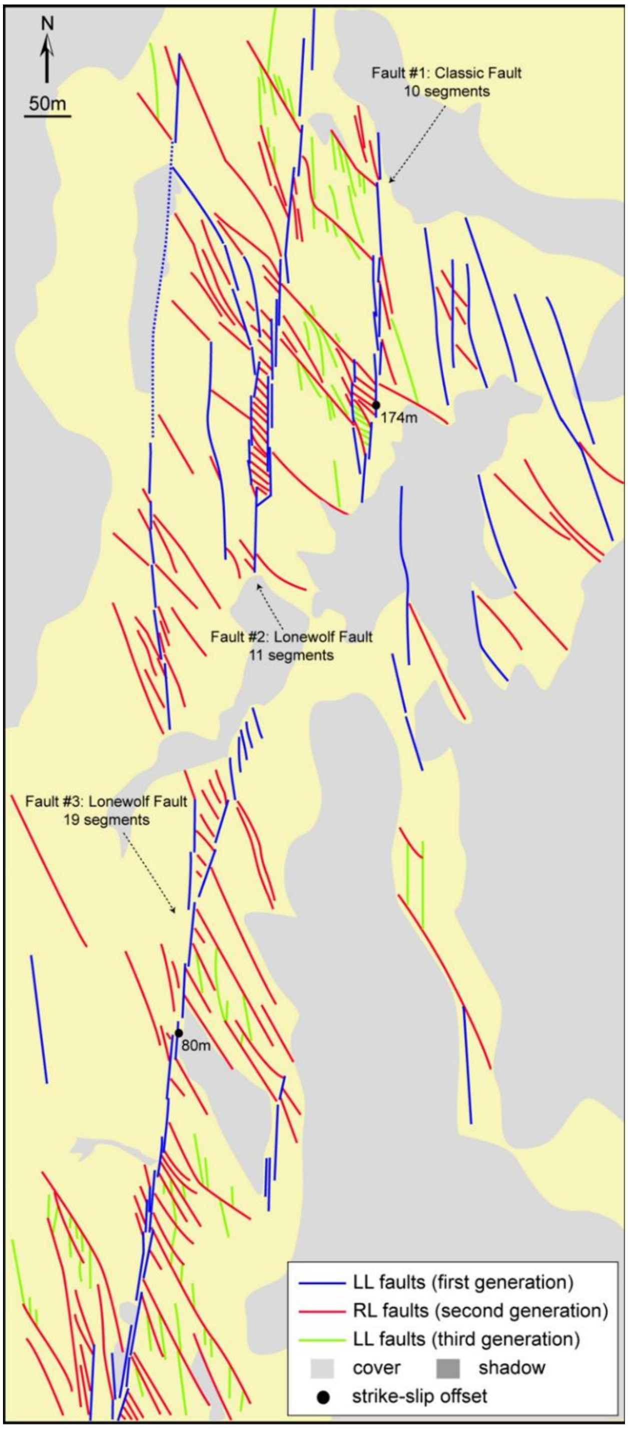

Figure 32 - Identification of fault segments along a primarily left-lateral strike-slip fault with over 80 m of slip. Blue lines are for left lateral (LL) fault traces and red lines for their splays, which later are often subjected to right-lateral (RL) shear. The fault traces are from Flodin and Aydin (2004) and the segment identification and interaction from de Joussineau and Aydin (2009).

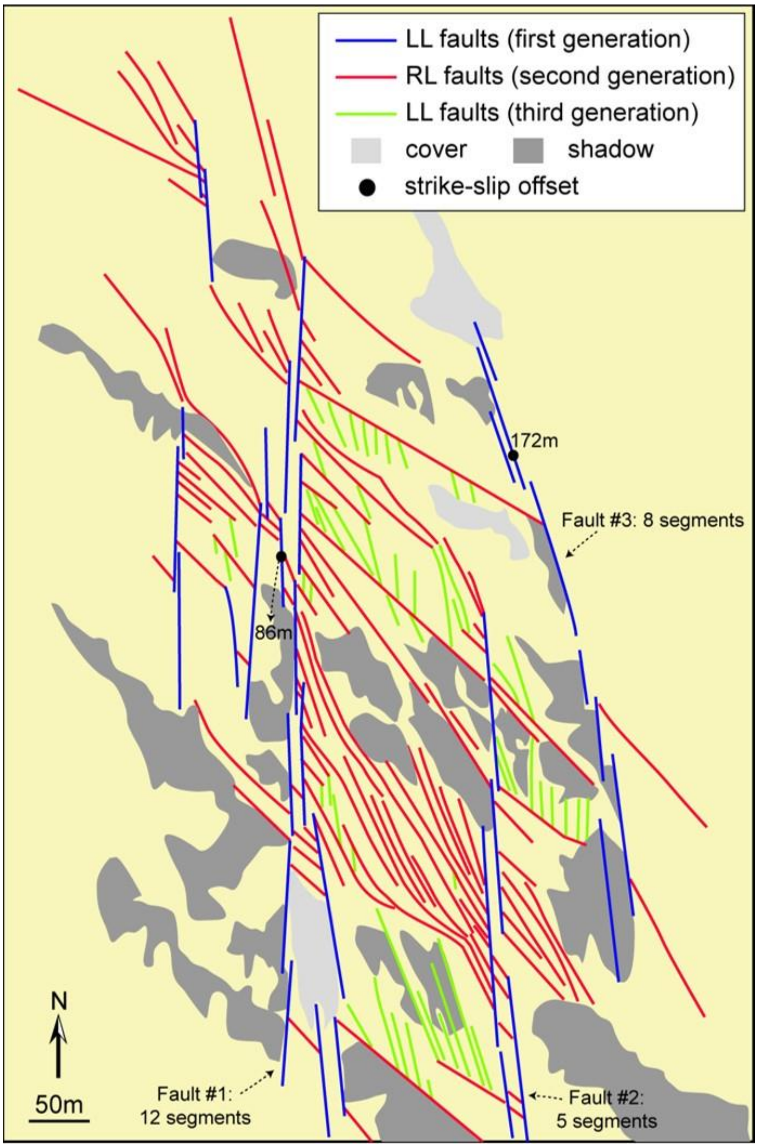

Figure 33 - Fault segments and their influence on the localization of the next generation of faults with specific kinematics. The map identifies fault segments (LL: left-lateral, RL: right-lateral) for deciphering and breaking down complex fault systems. Segment identification from de Joussineau and Aydin (2009).

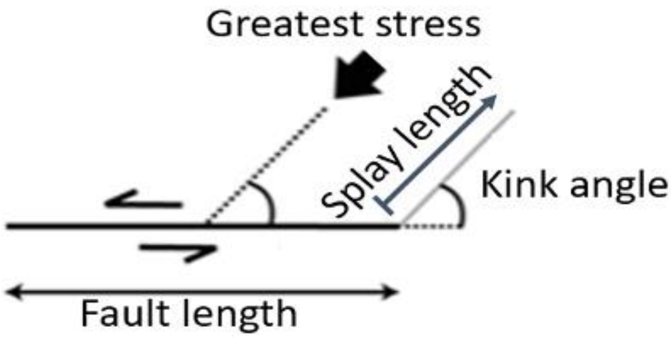

Figure 34 - Sketch defining parameters related to splay fractures. The fault and splay length are correlated: the longer the fault, the longer the splays. Modified from de Joussineau and others (2007).

The application of these concepts to field settings is not straightforward because fault growth is a continuous process. However, a field visit provides a snapshot of one instant in time that is the result of the full history. An analogy for reconstructing the fracturing history can be made to making a movie from still pictures of the system at discrete points in time.

Figure 32 is a map of a left-lateral fault with a little greater than 80 m offset (from Flodin and Aydin, 2004). The segments and the next generation of faults (i.e., those color-coded red) are due to shearing of the splays of the main segments with right lateral kinematics. The next generation of fractures, color-coded green in Figure 33, are the splays of the second-generation faults, which are better developed along faults labeled #1 and #2.

The impact of the fault networks presented in Figure 31, Figure 32 and Figure 33 on fluid flow is complex. The main fault segments and their largest splays typically accommodate meters to hundreds of meters of slip and have well-developed and continuous cores with low (cross-fault) permeability (Flodin et al., 2005). Consequently, they compartmentalize this reservoir. Their minor splays, however, are highly permeable open fractures enhancing the fluid flow. The largest of them could increase the connectivity of the fault networks at a scale of 100 m.

This process is also critical for normal fault patterns. For example, the Moab Fault (Figure 35) in Utah, USA, is a well-studied example in this category (Foxford et al., 1998; Davatzes et al., 2005). Figure 36, as compiled by Davatzes and others (2005), shows lateral relays (a and b, top) and a large intersection (b, bottom) along the Moab Fault and how these complexities control the nature and distribution of associated structures.

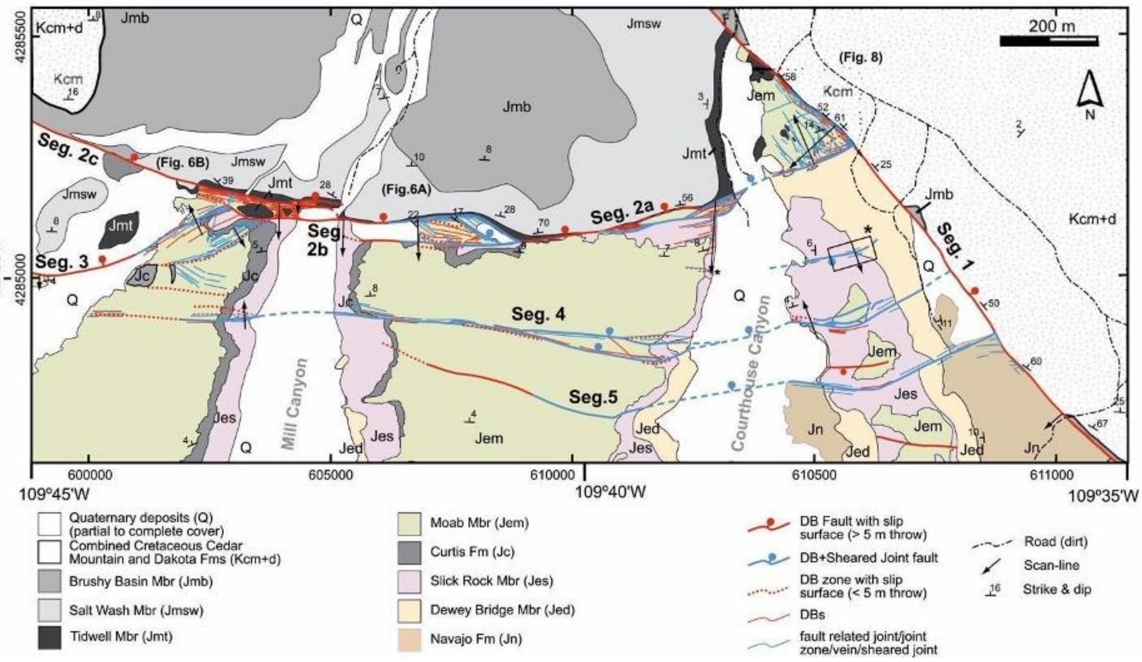

Figure 35 - Map showing the traces of the Moab Fault and its strands in southeast Utah. The Moab Fault is dominantly a normal fault with 900 m of maximum slip. Modified from Davatzes and others (2005).

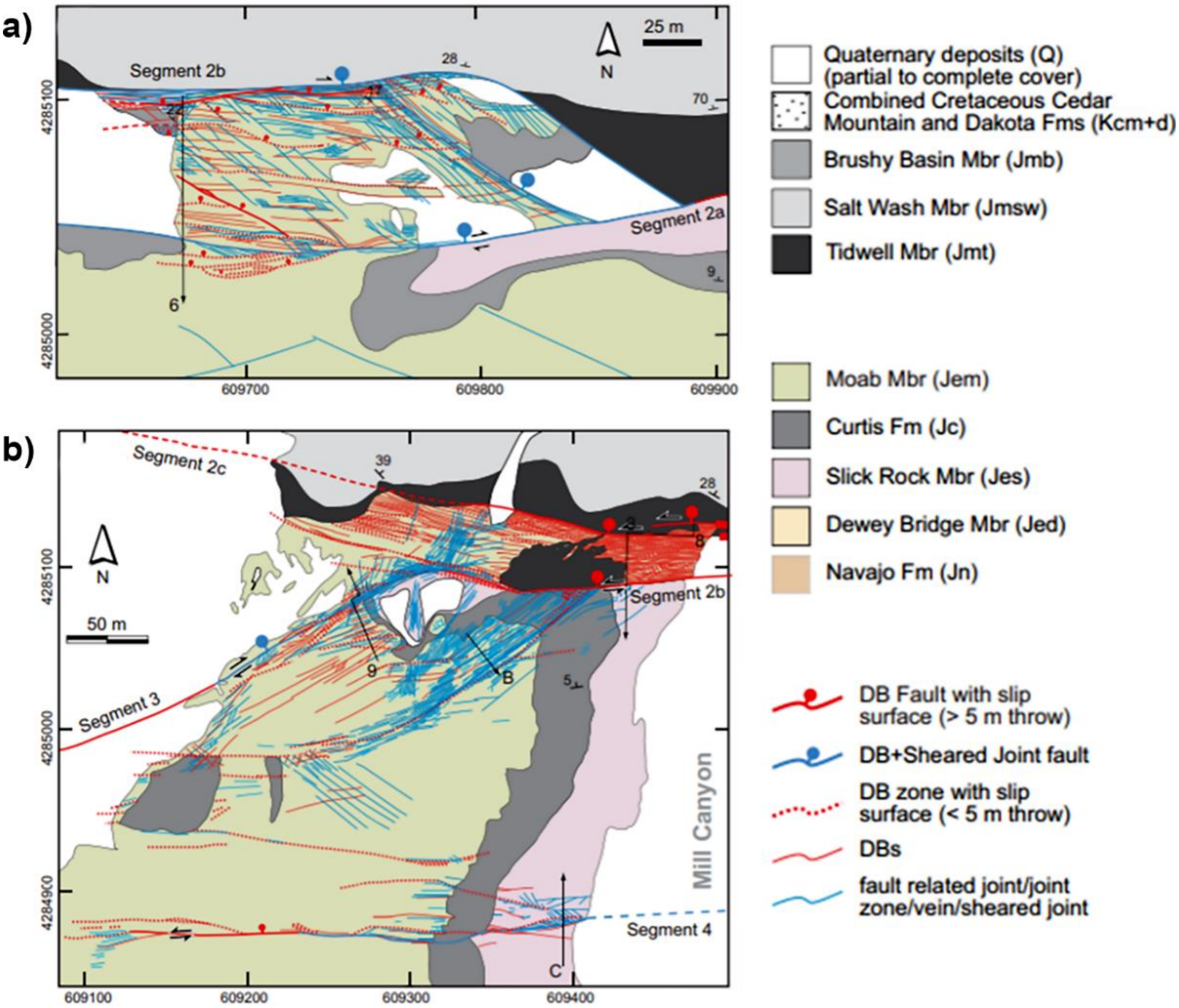

Figure 36 - Localization of deformation bands (DBs) and sheared joint type faults at lateral relays along the Moab Fault. The variation of the secondary structures appears to be a function of small components of strike-slip on the fault segments. a) Fault relay zone. b) Fault relay (top) and fault intersection (bottom) zones. Modified from Davatzes and others (2005).

12 Sandstone-Shale Sequences

Siliciclastic sequences commonly include alternating sandstone, siltstone and shale lithologies. Even small amounts of fine-grained materials, either silt or shale, have drastic consequences on deformation mechanisms due to the anisotropy they introduce and their greater ductility. This section provides examples of the role played by fine-grained lithologies on fracture occurrences, fracture terminations, fracture infill and shale entrainment.

Fine-grained units commonly occur at bedding interfaces and interdune boundaries. These have three important consequences.

1. They bound sandstone beds and dune packages as separate groundwater storage units because siltstones and shales are less permeable than sandstones. The fine-grained units act as aquitards (Aydin, 2014; Cilona at al., 2016).
2. They truncate joints and small faults (Helgeson and Aydin, 1991; Aydin and de Joussineau, 2014) and the fine-grained units compartmentalize aquifers.
3. Due to low shear strength, these units are prone to layer-parallel slip (Cooke et al., 2000) and they form fracture corridors in the adjacent sandstone units.

Sandstone packages or, morphologically speaking, tiers can be separated by fine-grained deposits at the flats, which are instrumental for demarcation of fracture systems in sandstone formations (Figure 37).

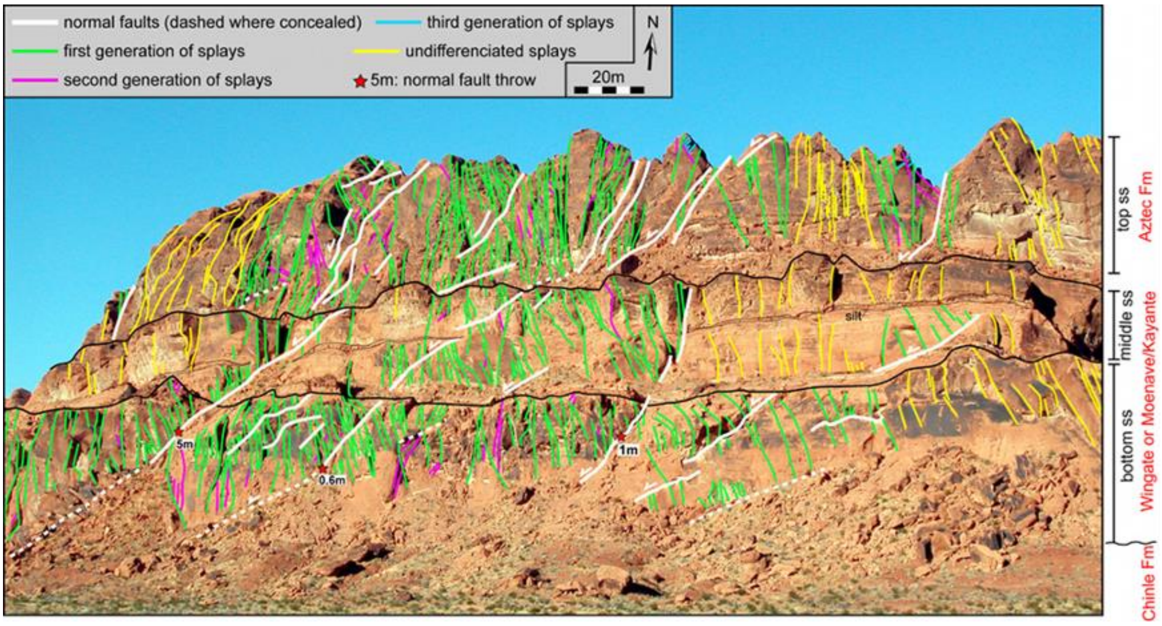

Figure 37 - A panoramic picture showing a cliff face about 200 m high exposing a series of Mesozoic sandstone formations with multiple generations of fractures including low-angle normal faults. Sandstone packages or, morphologically speaking, tiers are separated by fine-grained deposits, which are instrumental for demarcation of fracture systems in sandstone formations. The fracture systems are color-coded for their sequence of formation. Thick white lines show low-angle normal faults with small offsets. Slightly modified from de Joussineau and Aydin (2007b).

These units normally would be aquifers. Figure 38 and Figure 39 are isolated cases that better illustrate the role of fine-grained deposits in bounding fractured sandstone domains. Figure 38 shows an interdune deposit truncating a well-developed system of joints in sandstone units above the fine-grained deposits. Figure 39 shows slip across a fine-grained unit along a dune boundary (diagonal from lower right to upper left) with an associated joint cluster or corridor in the sandstone package (upper right).

Figure 38 - Photograph showing a fine-grained interdune deposit (indicated by blue lines) truncating a well-developed system of joints in the overlying Aztec Sandstone.

Figure 39 - Photograph showing slip across a fine-grained unit along an interdune boundary. The associated joint cluster in the sandstone package in the upper right with respect to interdune deposits indicates the presence of slip along the dune boundary.

13 Shale Entrapment into Fault Zones (Shale Smearing) and Flow Impact

The sketch and photograph (inset) in Figure 40 show the entrainment of shales into fault zones in an underground mine shaft in central California, USA. The sketch depicts a shale body (shale smear) about 1.6 m thick on the lower left, entrained along a normal fault of about 7 m offset (Eichhubl et al., 2005). Figure 41 shows sketches of smeared shales produced in the laboratory using sand and clay (Noorsalehi-Garakani et al., 2013; Vrolijk et al., 2016). The sketch in Figure 41b illustrates multiple shale layers entrained into the shear zone, similar to the natural example shown in Figure 40. Additional subsurface examples of shale entrainment are provided by Yielding and others (1997) and Koledoye and others (2003). Shale smears along faults may completely prevent fluids from flowing across the faults and may form major barriers to groundwater flow. In hydrocarbon exploration, fault smearing is one of the most common forms of traps in hanging walls of normal faults within sandstone-shale sequences.

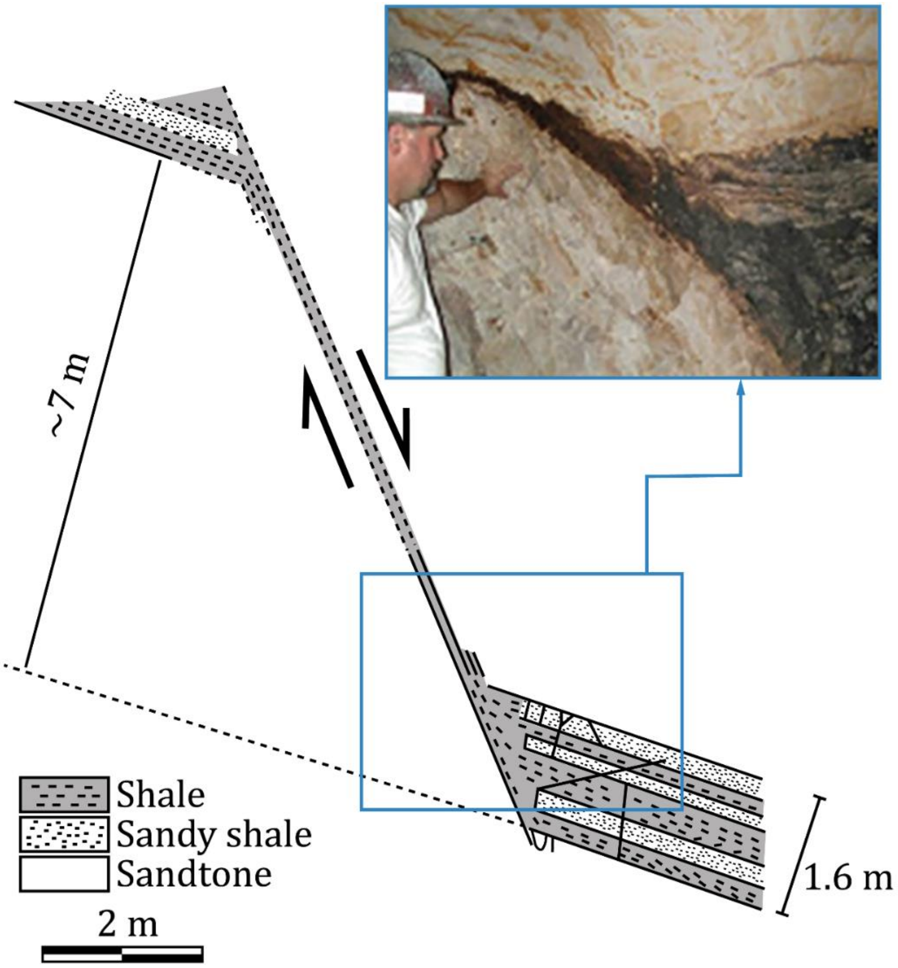

Figure 40 - Map and photograph showing shale entrained along a normal fault with a throw of 7 m in a mineshaft at Black Diamond Mine, California, USA. Modified from Eichhubl and others (2005).

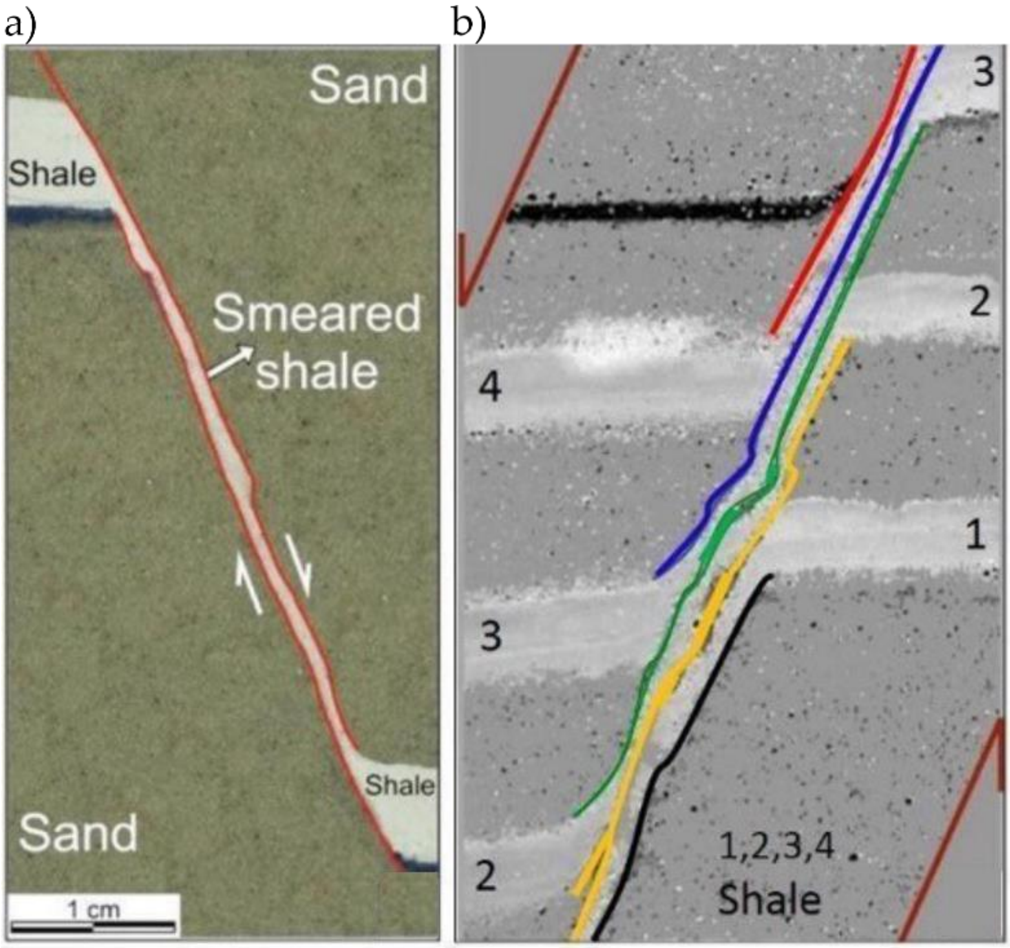

Figure 41 - Shale smear produced in experiments with sand and clay-like plaster in the laboratory by a) Noorsalehi-Garakani and others (2013); and, b) Vrolijk and others (2016).

When shale smearing occurs along a fault within an aquifer, it can cause a strong hydraulic head gradient across the fault as shown in the example of Figure 42 and Figure 43 from the Santa Susana Field Laboratory (SSFL) in Simi Valley, southern California, USA. Here shale is present along a fault zone called the Shear Zone Fault; its influence on groundwater flow is shown in Figure 43. Figure 43 indicates a difference of about 75 m in hydraulic head across this fault, which indicates the effective sealing behavior of the shale smear. See Box 3↴ for details.

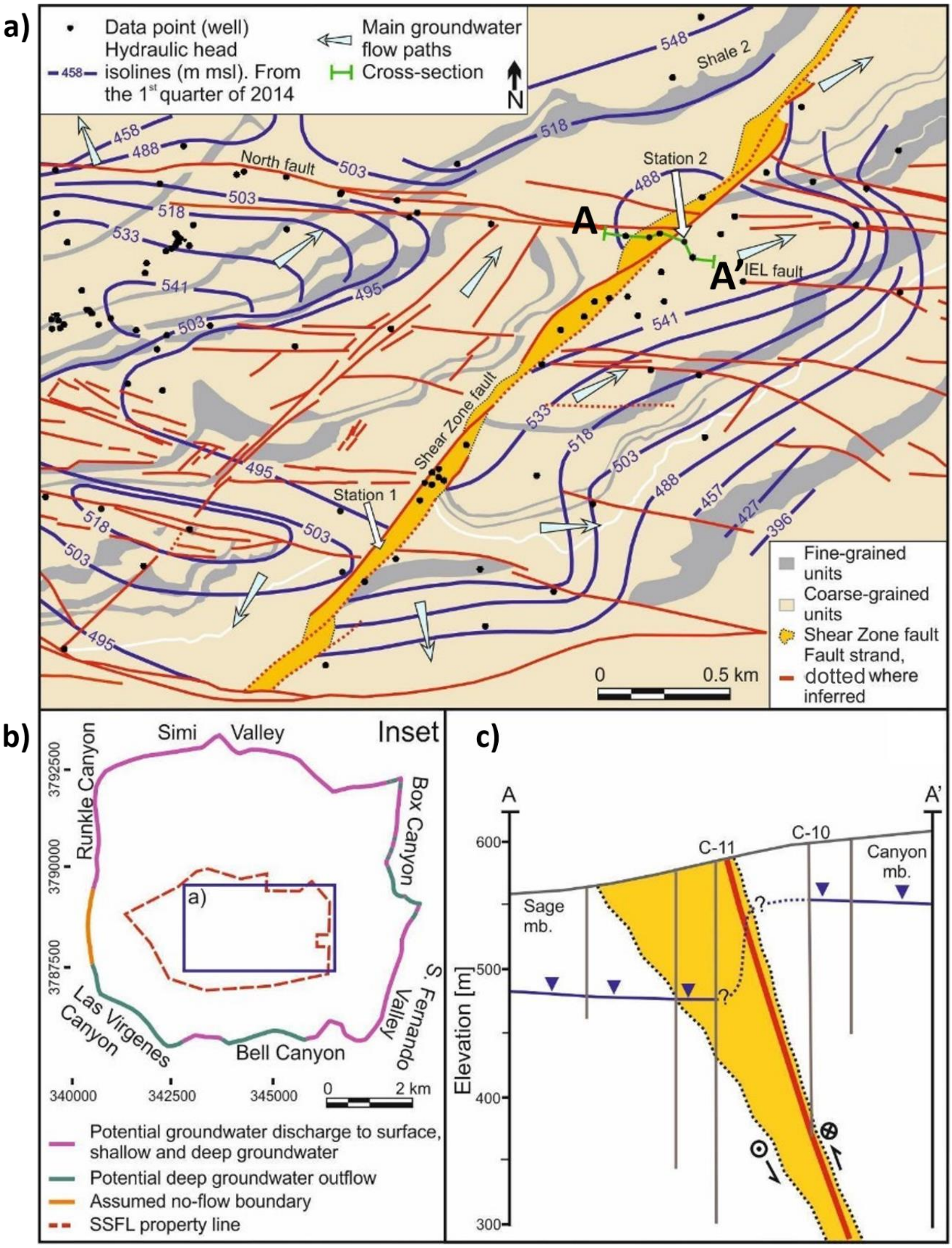

Figure 42 - Case study location. a) Hydrogeological map of the Santa Susana Field Laboratory which is the rectangular inset as indicated in b) that shows the area surrounding the Laboratory site, modified from MWH (Montgomery, Watson, and Harza) Global (2009 and 2014). The Shear Zone Fault is indicated in yellow, hydraulic head elevation by blue lines, and well locations by solid circles. c) Schematic cross-section A-A′ with the location indicated by a green line in (a), showing the hydraulic head drop recorded in five wells located along an approximately E-W direction on either side of the Shear Zone Fault. Modified from MWH (2009). The inferred kinematics of the fault zone (west side down and toward viewer) also are shown. Modified from Cilona and others (2015).

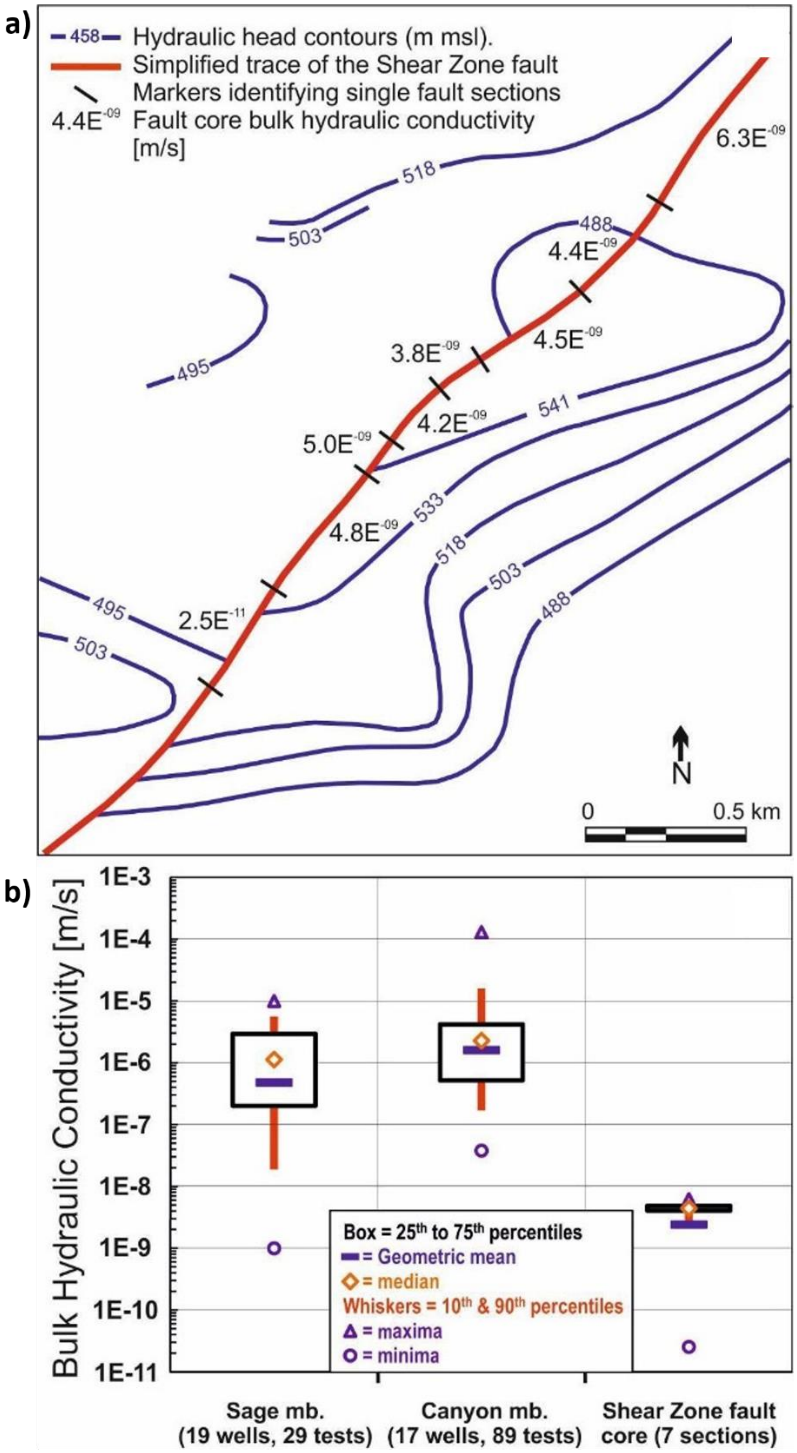

Figure 43 - Hydraulic head and hydraulic conductivity data for geologic features in the area (mb = member). a) Hydraulic head contours from the first quarter of 2014 are shown by blue lines, from MWH (2014). Representation of Shear-Zone Fault in the groundwater flow model is indicated by the red line and was redrawn from AquaResource/MWH (2007). Values of the hydraulic conductivity of the 6 m thick fault core are listed adjacent to each section of the fault, from AquaResource/MWH (2007). b) Box-and-whisker diagram of the hydraulic conductivity of the Shear Zone Fault and the surrounding sandstones, modified from Cilona and others (2015).

14 Wrap-up

This Groundwater Project book introduces the different kinds of fractures that occur in siliciclastic rocks, primarily in sandstone and with some consideration of the presence of interlayered shales, and the effect of these fractures on the flow of geofluids. The major fracture types and their occurrence in groups are described, and a few other classes that are considered rare in nature are mentioned. The references listed in this book provide more detailed information on this topic.

The overlying messages are that fracture types are widespread in siliciclastic rocks and these structural elements have a significant impact on groundwater flow. Almost every groundwater and contaminant transport problem in sandstone aquifers will involve complexities. It is best to be aware of them rather than assume the medium is homogeneous. The good news is that the heterogeneities imparted by these “fracture” features have been well studied at prototypical locations, which represent common tectonic and geological settings. The bad news is that other groundwater aquifers and their tectonic history are most likely different from those presented in this book. Therefore, the application of the results highlighted here to a specific groundwater environment may not be straightforward. However, understanding the deformation processes responsible for common fractures as well as their distribution and variability is useful when designing a strategy to deal with such issues in other settings.

There is a strong connection between structural heterogeneities and depositional heterogeneities including the most common one, bedding, particularly in the presence of fine-grained deposits such as shale or mudstone along the bedding interfaces and interdune boundaries in siliciclastic rocks. Most of the time, these cannot be resolved by seismic data or by investigating boreholes. Drilling is expensive so boreholes are sparse. That is why gathering basic knowledge of rock fracture from outcrops is one of the most affordable methods of assessing fracture heterogeneities and their potential impact on flow properties. When boreholes and/or seismic reflection data are available, the correlation of data from one borehole to another often hundreds of meters (sometimes several kilometers) apart or from one seismic reflection line to the next similarly far away is enhanced by knowledge about the potential fracture types, their architecture, their hierarchy, scaling relationships and petrophysical properties. It is a challenge to deal with these fracture properties in complex underground environments. This book provides examples of how to break down complex fracture systems by deciphering their components and how to understand the fracture systems by using the mechanical processes responsible for their progressive formation. It helps to keep in mind that everything in nature happens for a reason. It is up to the interpreter to discern the underlying processes that fractured the siliciclastic aquifer of interest. Thus, this book provides basic knowledge of fracture structures and their relationship to depositional fabric and mechanical processes that resulted in their formation.

Studies based on 3D and 4D modeling approaches are essential to the understanding and prediction of fracture and fault networks and should be used as soon as technology improves and new analysis tools become available. Such models would help in understanding not only fracture within small areas but also large-scale landscapes (Boersma et al., 2020).

Working with faults and fractures in geology applied to water flow and groundwater systems can be challenging because it is necessary to work with multiple mapping techniques and to call on more than one technical field such as mapping, structural geology, geochemistry and petrology (Laubach et al., 2018).

15 Exercises

Exercise 1

Fractures and faults are common structures in geology, and each kind of geological environment has specific controls on how these structures occur. Fractures and faults are important in groundwater flow systems as they often serve as primary flow pathways. The geology has a strong influence on the fracture network geometry and connectivity, and thus it is important to understand both the geology of the host rock and the fracture network to assess groundwater flow. The following diagram illustrates simplified kinematics for three fracture types.

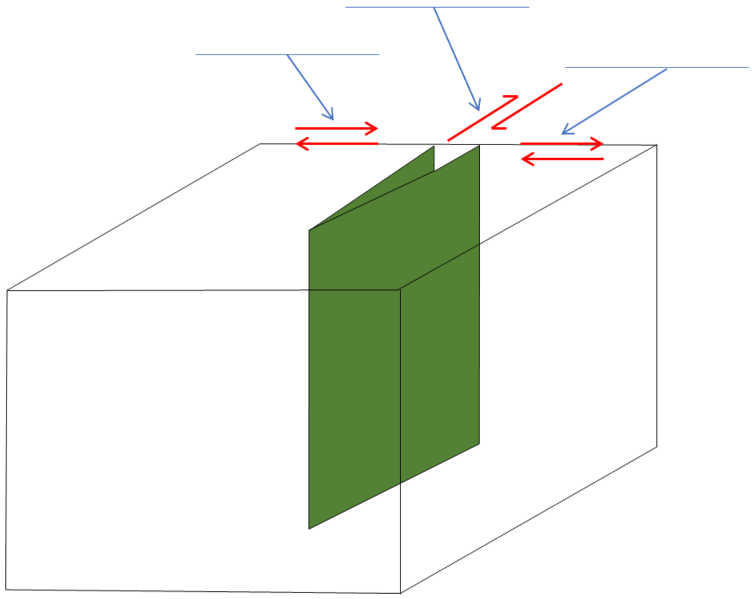

Schematic diagram showing basic kinematics of fractures

a) On the blue lines, correctly insert each kinematic type pointed to by the blue arrows.

b) Describe the type of fracture that forms from each of these three kinematic scenarios.

c) Using the relationship between two adjacent points of a fracture, describe the displacement discontinuity concept of S.L. Crouch (1976) that was presented in Figure 6.

Click for solution to Exercise 1⤵

Exercise 2

How can one distinguish between joints and shear fractures?

Click for solution to Exercise 2⤵

Exercise 3

Faults can have a strong influence on the flow system in fractured rock aquifers. Examine Figure 18 from Section 6.4. The following image is a version of Figure 18 from this book with the addition of a cross-section line A-A′ added perpendicular to the fault.

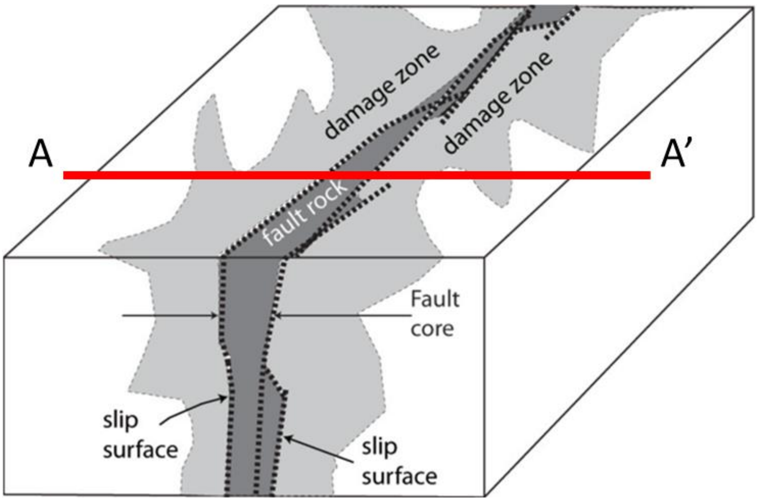

Idealized diagram showing fault zone elements: fault core, which includes fault rock and several slip surfaces, and surrounding damage zone, from Aydin and Berryman (2010).

a) Based on the following image and the description in Section 6.4, create a sketch showing the general permeability distribution along cross-section line A-A′. Section 13 of this book also provides useful information.

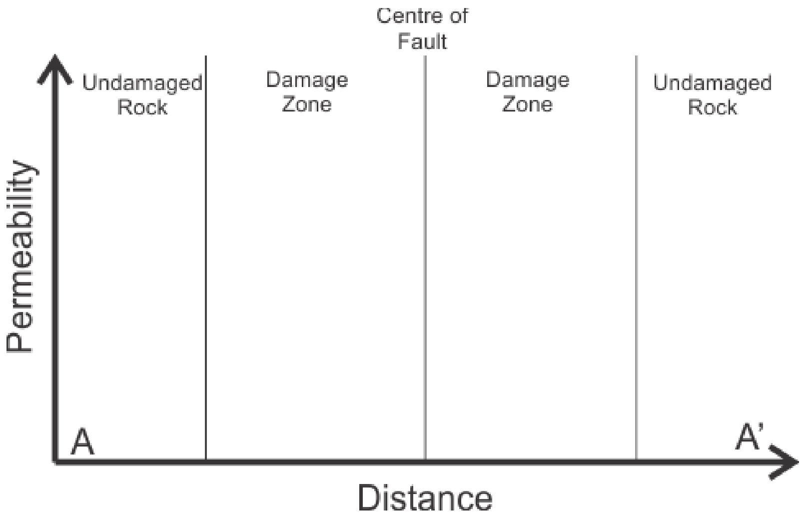

General permeability distribution along this cross-section line (A to A').

b) How might this permeability distribution influence the flow system? How might this distribution influence movement of contaminants?

Click for solution to Exercise 3

Exercise 4

The following image is a photograph of the Pirambóia Sandstone located in southern Brazil. The photograph was taken by Danilo Amendola in 2011 and donated to the authors for this book.

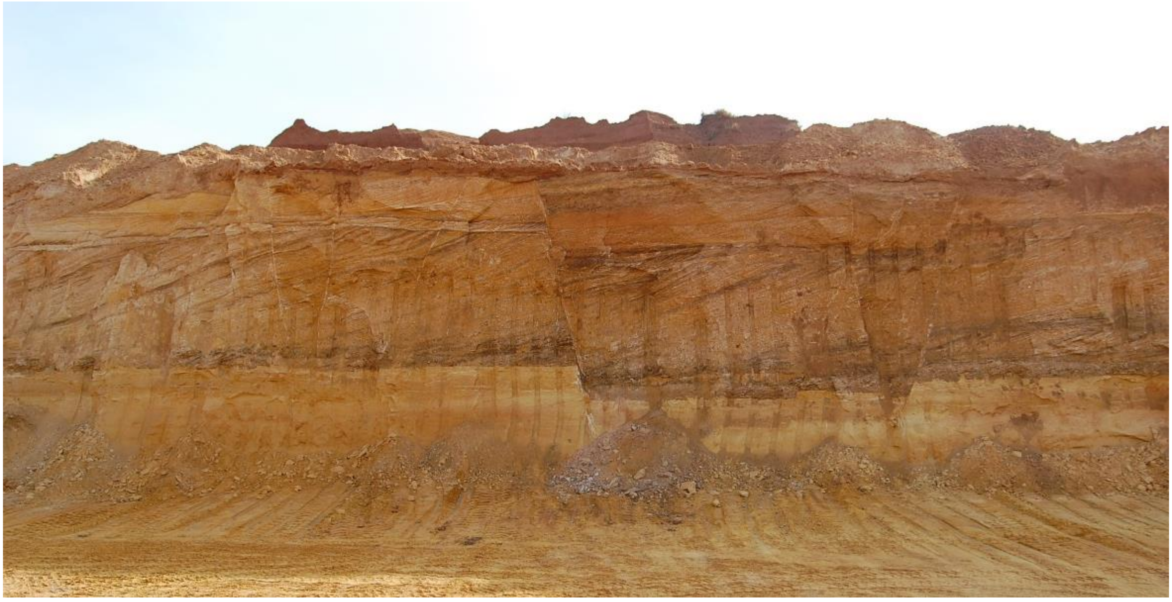

Pirambóia Sandstone located in southern Brazil. (Photograph by Danilo Amendola, 2011)

The Pirambóia Sandstone is an important aquifer in Brazil. This sandstone is well known as the major recharge source for the Guarani aquifer and has been intensively studied and cataloged across southern Brazil. Based on this picture, identify some of the predominant fracture/disconformity-related structures, and describe their potential importance for groundwater studies/dynamics.

Click for solution to Exercise 4⤵

16 References

Ahmadov, R., 2006, Petrophysics and permeability of fault zones in sandstone with a focus on fault slip surfaces and slip bands. Master of Science thesis, 85 pages, Stanford University, California, USA.

Ahmadov, R., A. Aydin, M. Karimi-Fard, and L. Durlofsky, 2007, Permeability upscaling of fault zones in the Aztec Sandstone, Valley of Fire State Park, Nevada with a focus on slip surfaces and slip bands. Hydrogeology Journal, volume 15, pages 1239-1250, doi: 10.1007/s10040-007-0180-2↗.

AquaResource, Inc/MWH, 2007, Three-dimensional groundwater flow model report. Santa Susana Field Laboratory, Ventura County, California, USA. AquaResource, Waterloo, Ontario, Canada.

Aydin, A. and A.M. Johnson, 1978, Development of faults as zones of deformation bands and as slip surfaces in sandstone. Pure and Applied Geophysics, volume 116, pages 931-942, doi: 10.1007/BF00876547↗.

Aydin, A. and J.G. Berryman, 2010, Analysis of the growth of strike-slip faults using effective medium theory. Journal of Structural Geology, volume 32, pages 1629-1642.

Aydin, A., 2014, Failure modes of shale and their implications for natural and man-made fracture assemblages. American Association of Petroleum Geologists Bulletin, volume 98, issue 11, pages 2391-2409, https://doi.org/10.1306/07311413112↗.

Aydin, A. and R. Ahmadov, 2009, Bed-parallel compaction bands in aeolian sandstone: their identification, characterization and implications. Tectonophysics, volume 479, issues 3-4, pages 277-284, doi: 10.1016/j.tecto.2009.08.033↗.

Aydin, A., R. Borja, and P. Eichhubl, 2006, Geological and mathematical framework for failure modes in granular rock. Journal of Structural Geology, volume 28, issue 1, pages 83-98, https://doi.org/10.1016/j.jsg.2005.07.008↗.

Aydin, A. and G. de Joussineau, 2014, The relationship between normal and strike-slip faults in Valley of Fire State Park, Nevada, and its implications for stress rotation and partitioning of deformation in the east-central Basin and Range. Journal of Structural Geology, volume 63, pages 12-26, http://dx.doi.org/10.1016/j.jsg.2014.02.006↗.

Aydin, A. and J. Zhong, 2017, Rock Fracture Knowledgebase. Harvard Dataverse, volume 1, http://library.rockfracture.com/Index.html↗.

Boersma, Q., W. Athmer, M. Haege, M. Etchebes, J. Haukås, and G. Bertotti, 2020, Natural fault and fracture network characterization for the southern Ekofisk field: a case list study integrating seismic attribute analysis with image log interpretation. Journal of Structural Geology, Volume 141, https://doi.org/10.1016/j.jsg.2020.104197↗.

Cashman, S. and K. Cashman, 2000, Cataclasis and deformation-band formation in unconsolidated marine terrace sand, Humboldt County, California. Geology, volume 28-2, pages 111–114, https://doi.org/10.1130/0091-7613(2000)28<111:CADFIU>2.0.CO;2↗.

Cherry, J.A., D. McWhorter, and B.L. Parker, Santa Susana Field Laboratory Groundwater Advisory Panel, 2009, *in* Conceptual Model for the Migration and Fate of Contaminants in Groundwater at the Santa Susana Field Laboratory, Simi, California (draft), volume 1-4, association with the University of Guelph, Montgomery Watson Harza, Haley and Aldrich, and AquaResource Inc (December), 448 pages, https://www.dtsc-ssfl.com/files/lib_rcra_groundwater/SWGWRIR/conceptualmodels/Vol%201%20of%204%20Draft%20SCM%20Dec%2009.pdf↗.

Cilona, A., A. Aydin, and N.M. Johnson, 2015, Permeability of a fault zone crosscutting a sequence of sandstones and shales and its influence on hydraulic head distribution in the Chatsworth Formation, California, United States of America. Hydrogeology Journal, volume 23, pages 405-419, http://dx.doi.org/10.1007/s10040-014-1206-1↗.

Cilona, A., A. Aydin, J. Likerman, B. Parker, and J. Cherry, 2016, Structural and statistical characterization of joints and multi-scale faults in an alternating sandstone and shale turbidite sequence at the Santa Susana Field Laboratory: implications for their effects on groundwater flow and contaminant transport. Journal of Structural Geology, volume 85, pages 95-114, https://doi.org/10.1016/j.jsg.2016.02.003↗.

Cooke, M., P. Mollema, D. Pollard, and A. Aydin, 2000, Interlayer slip and joint localization in the East Kaibab Monocline, Utah: field evidence and results from numerical modeling, *in* Forced Folds and Fractures, editors J.W. Cosgrove and M.S. Ameen, Geological Society, London, Special Publication, volume 169, pages 23-49.

Crouch, S.L., 1976, Solutions of plane elasticity problems by the displacement discontinuity method, Part I: infinite body solution. International Journal for Numerical Methods in Engineering, volume 10, pages 301-343, https://doi.org/10.1002/nme.1620100206↗.

Cruikshank, K. M., G. Zhao, and A.M. Johnson, 1991, Analysis of minor fractures associated with joints and faulted joints. Journal of Structural Geology, volume 13, pages 865-886, https://doi.org/10.1016/0191-8141(91)90083-U↗.

Cruikshank, K. M. and A. Aydin, 1995, Unweaving the joints in Entrada Sandstone, southwest limb of the Salt Valley anticline, Arches National Park, Utah, United States of America. Journal of Structural Geology, volume 17, pages 409-421, https://doi.org/10.1016/0191-8141(94)00061-4↗.

Davatzes, N.C. and P. Eichhubl, A. Aydin, 2005, Structural evolution of fault zones in sandstone by multiple deformation mechanisms: Moab fault, southeastern Utah. Geological Society of America Bulletin, volume 117, pages 135-148, https://doi.org/10.1130/B25473.1↗.

Davis, G.H., 1999, Structural geology of the Colorado Plateau region of southern Utah with special emphasis on deformation bands. Geological Society of America Special Paper, volume 342, 157 pages, https://doi.org/10.1130/SPE342↗.

de Joussineau, G., O. Mutlu, A. Aydin, and D.D., Pollard, 2007, Characterization of strike-slip fault-splay relationships in sandstone. Journal of Structural Geology, volume 29, pages 1831-1842, https://doi.org/10.1016/j.jsg.2007.08.006↗.

de Joussineau, G. and A. Aydin, 2007a, The evolution of the damage zone with fault growth in sandstone and its multiscale characteristics. Journal of Geophysical Research, volume 112, https://doi.org/10.1029/2006JB004711↗.

de Joussineau, G. and A. Aydin, 2007b, Normal faults as precursors to strike-slip faults networks in the Basin and Range province, Valley of Fire State Park, Nevada, United States of America. Stanford Digital Repository, 13 pages, http://purl.stanford.edu/jw080wt6699↗.

de Joussineau, G. and A. Aydin, 2009, Segmentation along strike-slip faults revisited *in* Mechanics, Structure and Evolution of Fault Zones, editors Y. Ben-Zion and C.G. Sammis. Pure and Applied Geophysics, pages 1575–1594, doi: 10.1007/978-3-0346-0138-2_3.↗.

de Joussineau, G. and J.P. Petit, 2021, Mechanical insights into the development of fracture corridors in layered rocks. Journal of Structural Geology, volume 144, https://doi.org/10.1016/j.jsg.2021.104278↗.

de Joussineau, G., 2023, The geometrical properties of fracture corridors. Tectonophysics, volume 586, https://doi.org/10.1016/j.tecto.2022.229637↗.

Deng, S. and A. Aydin, 2012, Distribution of compaction bands in 3D in an aeolian sandstone: the role of cross-bed orientation. Tectonophysics, volumes 574-575, pages 204–218, http://dx.doi.org/10.1016/j.tecto.2012.08.037↗.

Deng, S. and A. Aydin, 2015, The strength anisotropy of localized compaction: a model for the role of the nature and orientation of cross-beds on the orientation and distribution of compaction bands in 3-D. Journal of Geophysical Research, Solid Earth, volume 120, pages 1523-1542, doi:10.1002/2014JB011689↗.

Deng, S., A. Cilona, C. Morrow, C. Mapeli, C. Liu, D. Lockner, and M. Prasad, A. Aydin, 2015a, Cross-bedding related anisotropy and its interplay with various boundary conditions in the formation and orientation of joints in an aeolian sandstone. Journal of Structural Geology, volume 77, pages 175-190, https://doi.org/10.1016/j.jsg.2015.05.005↗.

Deng, S., L. Zuo, A. Aydin, J. Dvorkin, and T. Mukerji, 2015b, Permeability characterization of natural compaction bands using core flooding experiments and 3D image-based analysis: comparing and contrasting the results from two different methods. American Association of Petroleum Geologists Bulletin, volume 99, pages 27-49, http://dx.doi.org/10.1306/07071413211↗.

Deng, S., R. Jiang, M. Karimi-Fard, and A. Aydin, 2017, Fluid-flow effects of compartmentalized distribution of compaction bands in an aeolian sandstone in three dimensions. Petroleum Geoscience, volume 23, pages 223-230, https://doi.org/10.1144/petgeo2016-05↗.

Dippenaar, M., 2022, Original Figures Created for Fractures and Faults in Sandstone and Sandstone-Shale/Mudstone Sequences and Their Impact on Groundwater, Department of Engineering Geology and Hydrogeology, University of Pretoria, South Africa.

Du Bernard, X., P. Eichhubl, and A. Aydin, 2002, Dilation bands: a new form of localized failure in granular media. Geophysical Research Letters, volume 29, issue 24, pages 1-4, https://doi.org/10.1029/2002GL015966↗.

Dyer, J.R., 1983, Jointing in sandstone, Arches National Park, Utah. Doctor of Philosophy dissertation, Stanford University, California, USA, 212 pages, https://pangea.stanford.edu/research/srb/docs/theses/SRB_20_AUG83_Dyer.pdf↗.

Eichhubl, P., P.S. D'Onfro, A. Aydin, J. Waters, and D.K. McCarty, 2005, Structure, , petrophysics, and diagenesis of shale entrained along a normal fault at Black Diamond Mines, California - implications for fault seal. American Association of Petroleum Geologists Bulletin, volume 89, issue 9, pages 1113-1137, https://doi.org/10.1306/04220504099↗.

Eichhubl, P., J.N. Hooker, and S.E. Laubach, 2010, Pure and shear-enhanced compaction bands in Aztec Sandstone. Journal of Structural Geology, volume 32, pages 1873-1886, https://doi.org/10.1016/j.jsg.2010.02.004↗.

Flodin, E.A. and A. Aydin, 2004, Evolution of a strike-slip fault network, Valley of Fire State Park, southern Nevada. Geological Society of America Bulletin, volume 116, issue 1-2, pages 42-59, https://doi.org/10.1130/B25282.1↗.

Flodin, E.A., L.J Durlofsky, and A. Aydin, 2004, Upscaled models of flow and transport in faulted sandstone: boundary condition effects and explicit fracture modeling. Petroleum Geoscience, volume 10, pages 173-181, https://doi.org/10.1144/1354-079303-587↗.

Flodin, E.A., M. Gerdes, A. Aydin, and W.D Wiggins, 2005, Petrophysical properties and sealing capacity of fault rock from sheared-joint based faults, Aztec Sandstone, Nevada *in* Fault Seals and Petroleum Traps, editors R. Sorkhabi and Y. Tsuji. American Association of Petroleum Geologists Memoir, volume 85, pages 197-217, doi:10.1306/1033724M853136↗.

Fossen, H. R.A. Schultz, and A. Torabi, 2011, Conditions and implications for compaction band formation in the Navajo Sandstone, Utah. Journal of Structural Geology, volume 33, issue 10, pages 1477-1490, https://doi.org/10.1016/j.jsg.2011.08.001↗.

Foxford, K.A., J.J. Walsh, J. Watterson, I.R. Garden, S. Guscott, and S.D. Burley, 1998, Structure and content of the Moab Fault Zone, Utah, USA, and its implications for fault seal prediction. Geological Society of London Special Publication, volume 147, pages 87-103, https://doi.org/10.1144/GSL.SP.1998.147.01.06↗.

Guiheneuf, N., A. Dausse, J.R. de Dreuzy, and B.L. Parker, 2020, Flow-bearing structures of fractured rocks: Insights from hydraulic property scalings revealed by a pumping test. Accepted for publication in Journal of Hydrology, volume 598, doi: 10.1016/j.jhydrol.2020.125715↗.

Haimson, B. and J.W. Rudnicki, 2010, The effect of the intermediate principal stress on fault formation and fault angle in siltstone. Journal of Structural Geology, volume 32, pages 1701-1711, https://doi.org/10.1016/j.jsg.2009.08.017↗.

Helgeson, D.E. and A. Aydin, 1991, Characteristics of joint propagation across layer interfaces in sedimentary rocks. Journal of Structural Geology, volume 13, pages 897-911, https://doi.org/10.1016/0191-8141(91)90085-W↗.

Hill, R.E., 1989, Analysis of deformation bands in the Aztec Sandstone, Valley of Fire State Park, Nevada. Master of Science thesis, University of Nevada, Las Vegas, USA, 93 pages, https://digitalscholarship.unlv.edu/cgi/viewcontent.cgi?article=1075&context=rtds↗.

Jourde, H., E.A. Flodin, A. Aydin, L.J. Durlofsky, and X.H. Wen, 2002, Computing permeability of fault zones in eolian sandstone from outcrops measurements. American Association of Petroleum Geologists Bulletin, volume 86, pages 1187-1200, https://doi.org/10.1306/61EEDC4C-173E-11D7-8645000102C1865D↗.

Karimi-Fard, M., L. Durlofsky, and K. Aziz, 2004, An efficient discrete fracture model applicable for general purpose reservoir simulators. Science and Physics Education Journal, volume 9, issue 2, pages 227–236, https://doi.org/10.2118/88812-PA↗.

Keehm, T. Mukerji, and A. Nur, 2004, Permeability prediction from thin sections: 3D reconstruction and Lattice-Boltzmann flow simulation. Geophysical Research Letters, volume 31, https://doi.org/10.1029/2003GL018761↗.

Koledoye, B., A. Aydin, and E. May, 2003, A new process-based methodology for analysis of shale smear along normal faults in the Niger Delta. American Association of Petroleum Geologists Bulletin, volume 87, pages 445-463, https://doi.org/10.1306/08010200131↗.

Lachenbruch, A.H, 1961, Depth and spacing of tension cracks. Journal of Geophysical research, volume 66, pages 4273-4292, https://doi.org/10.1029/JZ066i012p04273↗.

Laubach, J.S.E., J. Lamarche, B.D.M Gauthier, W.M. Dunne, and J.S. David, 2018, Spatial arrangement of faults and opening-mode fractures. Journal of Structural Geology, volume 108, pages 2-15, https://doi.org/10.1016/j.jsg.2017.08.008↗.

Lenoir, N., J.E. Andrade, W.C. Sun, and J.W. Rudnicki, 2010, In Situ Permeability Measurements inside Compaction Bands Using X-Ray CT and Lattice Boltzmann Calculations. Advances in Computed Tomography for Geomaterials, https://doi.org/10.1002/9781118557723.CH33↗.

Liu, C., D.D. Pollard, A. Aydin, and S. Deng, 2015, Mechanism of formation of wiggly compaction bands in porous sandstone, volume 1. Observations and conceptual model. Journal of Geophysical Research, Solid Earth, volume 120, pages 8138-8152, https://doi.org/10.1002/2015JB012372↗.

Manzocchi, T., J.J. Walsh, P. Nell, and G. Yielding, 1999, Fault transmissibility multipliers for flow simulation models. Petroleum Geoscience, volume 5, pages 53-63, https://doi.org/10.1144/petgeo.5.1.53↗.

Meyer, J.R., B.L. Parker, and J.A. Cherry, 2014, Characteristics of high-resolution hydraulic head profiles and vertical gradients in fractured sedimentary rocks. Journal of Hydrology, volume 517, pages 27-44, https://doi.org/10.1016/j.jhydrol.2014.05.050↗.

Meyer, J.R., B.L. Parker, E. Arnaud, and A.C. Runkel, 2016, Combining high resolution vertical gradients and sequence stratigraphy to delineate hydrogeologic units for a contaminated sedimentary rock aquifer system. Journal of Hydrology, volume 534, pages 505-523, https://doi.org/10.1016/j.jhydrol.2016.01.015↗.

Mollema, P.N. and M.A. Antonellini, 1996, Compaction bands: a structural analog for anti-mode I cracks in aeolian sandstone. Tectonophysics, volume 267, pages 209-228, https://doi.org/10.1016/S0040-1951(96)00098-4↗.

MWH, 2009. Draft Site-wide Groundwater Remedial Investigation Report, Santa Susana Field Laboratory, Ventura County, California. Prepared for The Boeing Company, NASA, and U.S. DOE, December, volumes I-VII, 321 pages, https://www.dtsc-ssfl.com/files/lib_ceqa/ref_draft_peir/Chap3_ProjDesc/68557_MWH_2009b_Draft_Site_Wide_Groundwater_Remedial_Investigation_Report_1_Text.pdf↗.

MWH, 2014, Groundwater Monitoring Progress Report, First Quarter 2014, Santa Susana Field Laboratory, Ventura County, California. Prepared for The Boeing Company, NASA, and US DOE by MWH, Walnut Creek, California, USA, 426 pages, https://www.dtsc-ssfl.com/files/lib_rcra_groundwater/quarterly_an_gw_repo/annual/66565_2014_Annual_Report_GWM_Text,Tables,Figures.pdf↗.

Myers, R., 1997, Analysis of brittle deformation and permeability structure of cataclastic faults in porous sandstone. Stanford Digital Repository, 4 pages, http://purl.stanford.edu/vn095mt0105↗.

Myers, R. and A. Aydin, 2004, The evolution of faults formed by shearing across joint zones in sandstone. Journal of Structural Geology, volume 26, pages 947-966, https://doi.org/10.1016/j.jsg.2003.07.008↗.

Noorsalehi-Garakani, S., G.J. Kleine Vennekate, P. Vrolijk, and J. Urai, 2013, Clay-smear continuity and normal fault zone geometry - first results from excavated sandbox models. Journal of Structural Geology, volume 57, pages 58-80, https://doi.org/10.1016/j.jsg.2013.09.008↗.

Olson, J., 2004, Predicting fracture swarms - the influence of subcritical crack growth and the crack-tip process zone on joint spacing in rock *in* The Initiation, Propagation, and Arrest of Joints and Other Fractures. Geological Society of London Special Publication, volume 231, pages 73-87, https://doi.org/10.1144/GSL.SP.2004.231.01.05↗.

Olsson, W.A., J.C. Lorenz, and S. Cooper, 2004, A mechanical model for multiply-oriented conjugate deformation bands. Journal of Structural Geology, volume 26, pages 325-338, https://doi.org/10.1016/S0191-8141(03)00101-9↗.

Parker, B.L., J.A. Cherry, and S.W. Chapman, 2012, Discrete fracture network approach for studying contamination in fractured rock. AQUAmundi: Journal of Water Science, volume 60, pages 101-116, http://www.acquesotterranee.it/sites/default/files/Am06052.pdf↗.

Pollard, D.D. and A. Aydin, 1988, Progress in understanding jointing over the past century. Geological Society of America Bulletin, volume 100, pages 1181-1204, https://doi.org/10.1130/0016-7606(1988)100<1181:PIUJOT>2.3.CO;2↗.

Roznovsky, T. and A. Aydin, 2001, Concentration of shearing deformation related to changes in strike of monoclinal fold axis: the Waterpocket Monocline, Utah. Journal of Structural Geology, volume 23, pages 1567-1579, https://doi.org/10.1016/S0191-8141(01)00023-2↗.

Rudnicki, J. W. and J. R. Rice, 1975, Conditions for the localization of deformation in pressure-sensitive dilatant materials. Journal of the Mechanics and Physics of Solids, volume 23, pages 371-394, https://doi.org/10.1016/0022-5096(75)90001-0↗.

Schultz, R.S., 2019, Geological Fracture Mechanics. Cambridge University Press, https://doi.org/10.1017/9781316996737↗.

Shipton, Z.K., J.P. Evans, K.R. Robeson, C.B. Forster, and S. Snelgrove, 2002, Structural heterogeneity and permeability in faulted eolian sandstone: implications for subsurface modeling of faults. American Association of Petroleum Geologists Bulletin, volume 86, pages 863-883, https://doi.org/10.1306/61EEDBC0-173E-11D7-8645000102C1865D↗.

Spence, G.H., G.D. Couples, T.G. Bevan, R. Aguilera, J.W. Cosgrove, J.M. Daniel, and J. Redfern, 2014, Advances in the study of naturally fractured hydrocarbon reservoirs. The Geological Society of London Special Publication, volume 374.19, pages 1-22, http://dx.doi.org/10.1144/SP374.11↗.

Sterling, S.N., B.L. Parker, J.A Cherry, J.H. Williams, J.W. Lane Jr, and F.P. Haeni, 2005, Vertical cross contamination of trichloroethylene in a borehole in fractured sandstone. Ground Water, volume 43, issue 4, pages 557-573, https://doi.org/10.1111/j.1745-6584.2005.0087.x↗.

Sun, W.C., J.E. Andrade, J.W. Rudnicki, P. Eichhubl, 2011, Connecting microstructural attributes and permeability from 3D tomographic images of in situ shear-enhanced compaction bands using multiscale computations. Geophysical Research Letters, volume 38, issue 10, https://doi.org/10.1029/2011GL047683↗.

Torabi, A., A. Aydin, A. Cilona, B.E. Jarsto, and S. Deng, 2015, The dynamics and interaction of compaction bands in Valley of Fire State Park, Nevada, Unites States of America: implications for their growth, evolution, and geostatistical property. Tectonophysics, volume 657, pages 113-128, http://dx.doi.org/10.1016/j.tecto.2015.06.029↗.

Vrolijk, P., J.L. Urai, and M. Kettermann, 2016, Clay smear: review of mechanisms and applications. Journal of Structural Geology, volume 86, pages 95-152, https://doi.org/10.1016/j.jsg.2015.09.006

Wen, X.H., L.J. Durlofsky, and M. Edwards, 2003, Upscaling of channel systems in two dimensions using flow-based grids. Transport in Porous Media, volume 51, pages 343-366, doi: 10.1023/A:1022318926559↗.

Yielding, G., B. Freeman, and T. Needham, 1997, Quantitative fault seal prediction. American Association of Petroleum Geologists Bulletin, volume 81, pages 897-917, https://doi.org/10.1016/S0928-8937(97)80010-0↗.

Zhao, G. and A.M. Johnson, 1992, Sequence of deformations recorded in joints and faults, Arches National Park, Utah. Journal of Structural Geology, volume 14, pages 225-236, https://doi.org/10.1016/0191-8141(92)90059-6↗.

Zhong, J., A. Aydin, and D.L. McGuinness, 2009, Ontology of fractures, Journal of Structural Geology, volume 31, pages 251-259, https://doi.org/10.1016/j.jsg.2009.01.008↗.

17 Boxes

Box 1 Splay Fractures Associated with Strike-slip Faults and Their Properties

This box highlights the length and angular characteristics of splays associated with strike-slip faults, along with their controlling parameters, primarily from de Joussineau and others (2007). These geometrical characteristics are relevant for groundwater flow in aquifers as they govern the distance at which splays extend from their parent faults and their angle to them. There is a clear positive correlation between the splay length and the parent fault length: the longer the fault, the longer the splays. The splay length also depends on the remote principal stress ratio: it increases with increasing stress ratio.

The angle that splays make with their parent fault, called the kink angle, depends on the fault configuration and the stress regime. If faults are isolated, their splays make a small angle with the parent fault, typically on the order of 20-30°. Conversely, if faults are located close to one another and could mechanically interact, the splays tend to form at a higher angle with their parent fault, typically above 40°. Finally, as is the case for splay length, the stress regime acting at the time of formation of splays impacts their angular relationships with their parent fault. A wide range of kink angles is possible depending on the confining pressure, the principal stress ratio and the angle of the parent fault with the maximum principal stress.

Return to where text linked to Box 1↥

Box 2 Properties of Slip Bands

Scanning electron microscopy analyses of slip band infill along three transects showed strong peaks in Fe-rich mineral cement (goethite/hematite mixture) and a corresponding decrease in Si- and O_2-rich mineral cement. The X-ray diffraction analyses of the samples with a whitish infill showed a strong peak corresponding to amorphous silica, which is believed to be opal. Opal as well as goethite/hematite infill markedly reduce the porosity and permeability of slip bands. Permeability values of slip bands partially filled with hematite/goethite cement were computed using thin-section image analyses in conjunction with a computational rock physics-based algorithm called PETS (permeability estimation from thin sections) and the Lattice-Boltzmann method (Keehm et al., 2004). Slip band permeabilities are commonly expressed in millidarcies (mD) and are estimated to be in the range of 7×10^{-6} mD to 3.9 mD. Partially filled slip band permeabilities range from 2.8 mD to 150 mD, whereas open slip surfaces have permeabilities as high as 5×10^{6} mD.

Return to where text linked to Box 2↥

Box 3 Outcomes from the Santa Susana Field Laboratory

At the Santa Susana Field Laboratory (SSFL) in California, USA, intensive subsurface investigation of groundwater contamination in the local sedimentary bedrock has been conducted since the 1980s, and field-based research has been undertaken since the mid-1990s. The bedrock is dominated by sandstones with lesser siltstones and conglomerates interbedded with shales. This site is the perfect field laboratory to study how faults and fractures impact groundwater flow and contaminant transport given multiple high-resolution data sets. Indeed, numerous cored boreholes and an extensive groundwater monitoring network consisting of conventional wells and depth-discrete multilevel systems, along with geophysical tools and structural geology analysis, have been used to understand the hydrogeologic conditions governing the migration of contaminants, with trichloroethylene being of primary interest (Sterling et al., 2005; Cherry et al., 2009; Meyer et al., 2014).

At this location, groundwater flow occurs almost entirely in the fractures because the rock matrix has low permeability (Parker et al., 2012). Well data suggest that hydraulically active fractures are present nearly everywhere at SSFL and, together with larger faults, create an interconnected network of fractures of variable length and aperture that determine the rate and direction of flow and influence the nature of the contaminant plume (Cherry et al., 2009; Guiheneuf et al., 2020). Fault zones at SSFL have contrasting hydraulic behavior: some are barriers to cross-flow, whereas others are conduits (Figure 42 of this book). Cilona and others (2015) focused on the mechanisms responsible for the barrier behavior and its impact on contaminant transport. Guiheneuf and others (2020) showed the variability of hydraulic response behavior in multiple observation wells in the area shown in Figure 42a; this behavior depended on the depth interval of the monitoring intervals and on the intersection with the larger-aperture and longer fractures associated with the Shear Zone Fault, given the location of the pumping well within the orthogonal IEL fault (shown in Figure 42a). As shown in Figure 42c, groundwater levels differ by as much as 75 m across a major NE-SW striking Shear Zone Fault zone. The hydraulic heads on the southeast side of this fault are systematically higher than those on the northwest side. Despite this strong NW-SE (fault-perpendicular) groundwater hydraulic gradient, the migration of contaminant plumes is significantly restricted from east to west across this fault (Cherry et al., 2009), and the concentration of contaminants suggests that the plume southeast of the fault is elongated parallel to fault strike (Cherry et al., 2009). These observations are consistent with the hydraulic conductivity of the fault core, which was estimated to be more than two orders of magnitude lower than the bulk hydraulic conductivities of surrounding sandstone units, based on the geometric mean and median values of multiple measurements (Figure 43a,b).

The model that was proposed to explain the barrier effect of the Shear Zone Fault involves the presence of deformed shales in the fault core, which were incorporated into the fault zone by a mechanism known as shale smearing. In this mechanism, the platy clay minerals of shales are re-aligned parallel to the shear direction resulting in reduced hydraulic conductivity of the deformed shale along the fault zone that generates strong contrasts in hydraulic conductivity along the zone. The resultant anisotropy in hydraulic conductivity influences groundwater flow.

Return to where text linked to Box 3⮥

18 Exercise Solutions

Solution Exercise 1

a) The labeled blue lines are shown below.

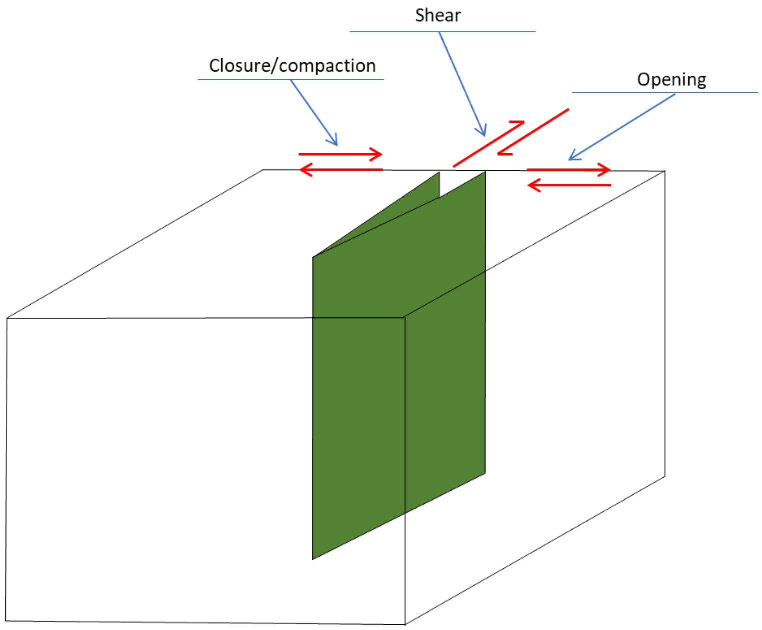

b) Closure/compaction would lead to pressure solution seams and shearing mode fractures; opening mode would lead to joints, and shearing mode would lead to shear fractures or faults.

c) The difference in the displacement of adjacent points on the two faces of a fracture defines the displacement discontinuity, which is related to the kinematics of the movement. Thus, by analyzing the fractures one can define not only their formation but also their behavior through time. Following S.L. Crouch (1976), displacements along each fracture face may be assumed to be positive in the positive coordinate directions. Then, displacement discontinuity normal to the fracture $D_n = U_y^+ - U_y^-$ defines an opening if positive and a closing if negative. Displacement discontinuity parallel to the fracture $D_s = U_x^+ - U_x^-$ denotes shear displacement discontinuity.

Return to Exercise 1↥

Solution Exercise 2

Shear fractures and faults can be identified by the presence of the offset of a marker bed on either side of the fracture that was continuous before the shearing motion. Faults often have nearly planar surfaces with a polished appearance and striations and grooves formed in the direction of slip. Although offset marker horizons can indicate that shearing has occurred, for defining the mechanism of faulting and kinematic vectors (fault slip direction), the planar fault surface and striations/grooves on the fault surface must be examined. If there is no evidence of these shear indicators, the discontinuity is likely a joint where the subparallel fracture walls moved away from one another without an offset (opening fracture).

The image below provides an example of offset marker horizons.

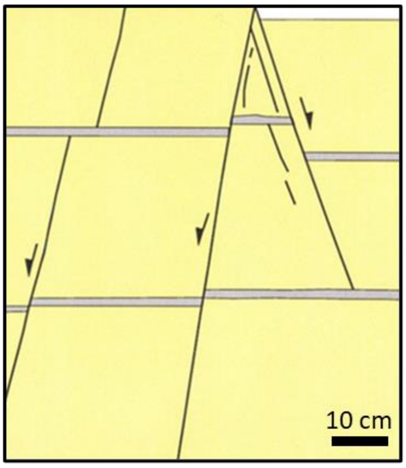

Return to Exercise 2↥

Solution Exercise 3

a) The permeability distribution across a fault varies considerably, as described in the text. The highest permeability will be in the damage zone that flanks both sides of the fault core, due to the abundant fractures in this zone. The fault core typically has a low permeability from crushing and smearing of fine-grained sediment (e.g., shales).

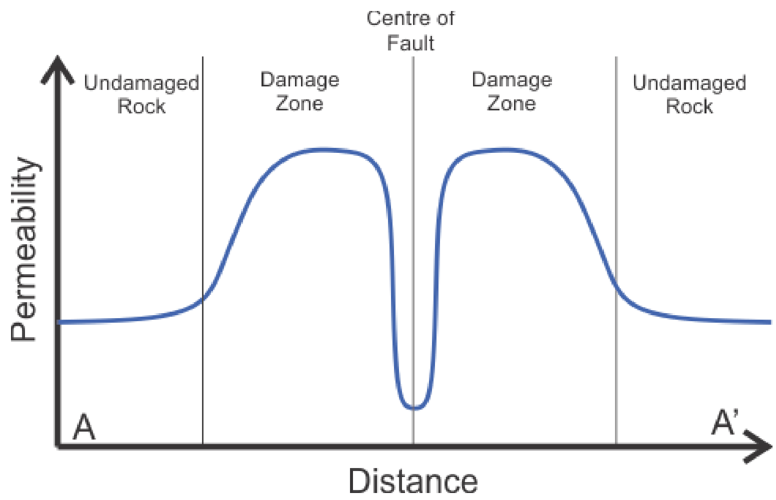

b) The permeability variations may have significant influence on the flow system. Major preferential flow pathways can occur on either side of the fault within the damage zone because the permeability there is typically much higher than that of the undamaged host rock. The fault core typically has a very low permeability and thus can act as a barrier to flow. This can compartmentalize the flow system into distinct hydrogeological units across the fault. If this were at a contaminated site, the mass flux of contaminants (i.e., the amount of contaminant being transported by the flowing water) could be significantly higher in the damage zone. In contrast, the low-permeability fault core may serve as a barrier to contaminant migration (across the fault). Thus, it is critical to characterize the physical and hydraulic character of faults as part of a hydrogeological investigation in fractured rock.

Return to Exercise 3↥

Solution Exercise 4

Although it can be difficult to observe every important feature at this scale, some obvious structures stand out. In the photograph below, many of the regularly spaced vertical striations on the cliff are the result of digging/quarrying and do not reflect natural features.

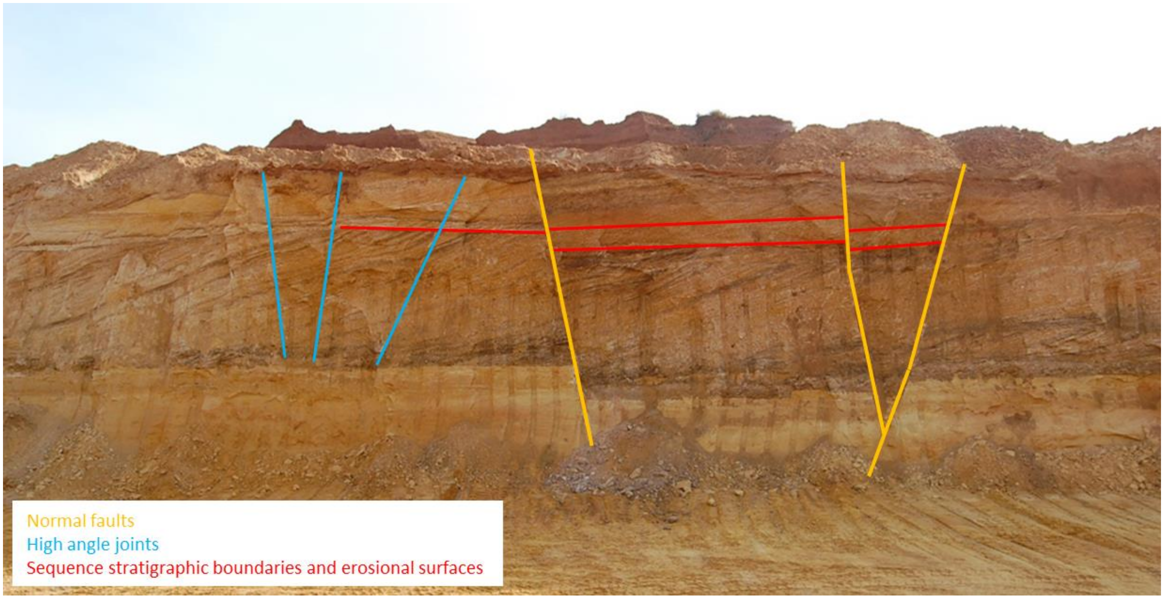

The photograph shows some excellent examples of normal faults (highlighted in orange), the offset of which can be observed by the displacement of several marker beds. On the left-hand side, some larger high-angle joints are visible, which may be important pathways for groundwater and recharge. Many more fractures exist but are not visible at this scale.

Sedimentary structures such as cross-beds are also visible as the diagonally dipping beds in the center of the exposure. These structures can provide insight into the flow direction and environment during deposition. They may also affect fracture orientations and propagations, and the mechanical properties of the rock sometimes change from bed to bed.

Finally, several sequence stratigraphic boundaries and erosional surfaces (angular unconformities and disconformities) can be observed in the photograph, such as the boundaries at the top and bottom of the cross-bedded unit. Some are highlighted in red. These surfaces can also introduce significant mechanical contrasts in the rock sequence that can impact fracture propagation and connectivity. They have also been linked to hydrogeological unit boundaries in other sedimentary rock aquifers (Meyer et al., 2016).

Return to Exercise 4↥

19 About the Authors

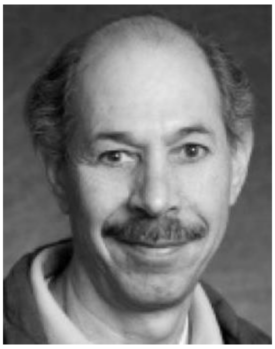

Dr. Atilla Aydin was born in a small village in eastern Turkey. Partly because of his good luck, he received his Bachelor of Science degree in geological engineering from Istanbul Technical University (Turkey) and Master of Science and Doctor of Philosophy degrees in geology from Stanford University (California, USA). He taught Structural Geology for about 10 years at Purdue University (Indiana, USA) and a graduate course titled "Faults, Fractures, and Fluid Flow" at Stanford University for about two decades. The latter led to the inception of this Knowledgebase. He is the author or co-author of more than 140 refereed papers, the references for which can be found here↗. Atilla was the co-founder and co-director of the Rock Fracture Project and the founder and director of the Shale Smear Project at Stanford University. Many field trip guidebooks and numerous workshop volumes from these projects are now available in digital (pdf) format from the Rock Fracture Project and Shale Smear Project data repositories of the Stanford University Library. He was Emeritus Professor of Research at the Department of Geological Sciences at Stanford until his passing on February 8, 2022.

Dr. Ramil Ahmadov, is an integrated geoscientist with 15+ years of experience in conducting pure and applied research in geoscience and engineering who has held various roles at BP, Ikon Science, New England Research and CGG. Dr. Ahmadov has considerable experience integrating laboratory, well log, seismic and production data within integrated multidisciplinary teams at all stages from exploration and development to production. Ramil holds Doctor of Philosophy and Master of Science degrees in geophysics and geology from Stanford University, a Master of Science degree in petroleum engineering from University of Wyoming and a Bachelor of Science degree in petroleum engineering from Azerbaijan State Oil Academy.

Dr. Marco Antonellini is a professor in the Department of Biological, Geological, and Environmental Sciences at the University of Bologna. He has a Bachelor of Science in earth sciences from the University of Bologna (Italy), a Master of Science in geology from Michigan State University, and a Doctor of Philosophy in quantitative structural geology from Stanford University (USA). His current research concerns structural geology and coastal hydrogeology. The main interests include fluid-rock interactions in deformed rocks, salt-water intrusion in coastal aquifers, relationships between geological structures and karst development, and water resources management. At present, his students work on the deformation of carbonate rocks, on the processes relating deformation and diagenesis, and on salt-water intrusion in mechanically drained coastal basins. He has authored more than 150 scientific contributions, is involved in national and international research projects, and collaborates with prestigious international institutions.

Dr. John Cherry, after studying in the USA and being a post-doctoral student in France, joined the University of Waterloo (Canada) in 1971 for field research on the migration and fate of contaminants in groundwater and their remediation. He co-authored *Groundwater* with R.A. Freeze (1979) and co-edited/co-authored several chapters in the book *Dense Chlorinated Solvents in Groundwater* (1996). He is the founding director of the University Consortium for Field-Focused Groundwater Contamination Research. At the G360 Centre for Groundwater Research, University of Guelph (Canada), he participates in research on groundwater monitoring technologies and creating safe wells for rural people in remote terrain. He was Chair of the Canadian Expert Panel on Environmental Impacts of Shale Gas Development (2012, 2014). He is a Foreign Member of the U.S. Academy of Engineering. He received the Lee Kwan Yew Water Prize in 2016 and the Stockholm Water Prize in 2020.

Dr. Antonino Cilona, has a Doctor of Philosophy in structural geology and rock mechanics from the University of Camerino (Italy) and undertook post-doctoral study at Stanford University. He is passionate about brittle deformation and the impact of faults and fractures on fluid flow. Since 2015 he has worked for Shell Global Solutions International B.V. where he focuses on fault seal, fluid-rock interaction, and new machine learning techniques to interpret fractures and pore types from different types of images.

Dr. Shang Deng received a Bachelor of Science degree (2010) in geology (with Honors) from Moscow University (Russia). He graduated from the Structural Geology and Geomechanics Graduate Program at Stanford University and received his Doctor of Philosophy degree in 2014. Before joining Sinopec, he worked for the Structure & Geomechanics group led by Peter Hennings at ConocoPhillips, Houston, from 2014 to 2015. His subjects of interest include mechanics of faults and fractures and their influence on hydrocarbon migration and accumulation in deep-buried carbonates. He is a structural geologist engaged in Shunbei oilfield exploration in the Tarim Basin and a senior engineer in Ma Yongsheng's laboratory.

Dr. Eric Flodin is currently an earth science advisor with Chevron at Cabinda Gas and Oil Company in Luanda, Angola. Prior roles include petroleum development geology at Tengizchevroil and Chevron Indonesia Sumatra Operations; characterization, modeling, and simulation at Chevron Technology Company; and as faculty in the Geosciences Department at Indiana-Purdue Fort Wayne. Eric holds a Bachelor of Science degree in geology from Indiana-Purdue Indianapolis and a Doctor of Philosophy in geology from Stanford University.

Dr. Ghislain de Joussineau is the Director of Technology & Operations at Beicip-Franlab, the consultancy branch of the French Institute of Petroleum and New Energies. After obtaining a Doctor of Philosophy in structural geology from the University of Montpellier (France), he joined the Rock Fracture Project at Stanford University (USA) as a post-doctoral student working with Professor Atilla Aydin. His research in both institutes was focused on the mechanisms of development and fluid flow properties of faults and fractures in rocks. He joined Beicip-Franlab in 2007 as a consultant and subsurface project manager. He then led the team in charge of the development of naturally fractured reservoirs for five years, before managing the Reservoir Engineering Department of the company. In 2019, he was appointed Director of Technology and Operations and member of the Executive Committee of Beicip-Franlab, before joining its Management Board in 2021 In this position, he oversees the implementation of consultancy and software development projects and the definition and realization of innovation programs.

Dr. Beth L. Parker holds a Natural Sciences and Engineering Research Council Industrial Chair in Groundwater Contamination, is a professor in the School of Engineering, and is the Founding Director of the G360 Institute for Groundwater Research, all at the University of Guelph (Canada). Dr. Parker is an internationally recognized expert in contaminant hydrogeology and groundwater flow system characterization and monitoring. She has made exceptional contributions to the understanding and remediation of contaminated groundwater, with a focus on fractured media, especially the role of diffusion on contaminant movement, attenuation, and remediation performance. Her research has profoundly changed the scientific understanding of how contaminants travel through bedrock to pollute freshwater resources and of the characteristics of aquitards providing source water protection, with field experience in North America, Latin America, and several European countries. Her research emphasizes field methods and a systems approach to understanding groundwater flow systems, contaminant transport and fate, groundwater monitoring and vulnerability assessments, groundwater remediation, sustainable groundwater use, multiphase fluid flow, and vadose zone/recharge. Dr. Parker has received the John Hem award (2009) and the M. King Hubbert award (2018) from the National Ground Water Association, a fellowship in the American Geophysical Union (2019), and recognition from the American Academy of Environmental Engineers & Scientists as a Board-Certified Environmental Engineering Member (2020); she became a Canadian Academy of Engineering Fellow in 2021.

Dr. Jian Zhong, received her Master of Science degree in geoscience and computer science from the State University of New York Stony Brook and her Doctor of Philosophy degree in geology from Stanford University. Her dissertation was focused on ontology application and knowledge representation in structural geology. She is a co-author of the Rock Fracture Knowledgebase.

Please consider signing up for the GW-Project mailing list to stay informed about new book releases, events and ways to participate in the GW-Project. When you sign up for our email list, it helps us build a global groundwater community. Sign up↗.

THE GROUNDWATER PROJECT

Modifications to Original Release

Changes from the Original Version to Version 2

Original Version: 17 January 2023, Version 2: 24 January 2023

Page numbers refer to page numbers in the original pdf.

Specific changes:

page 8, added scale to Figure 9

page 9, changed 'Figure 10a' to 'Figure 9a' in the second to last sentence in the second paragraph

page 12, added q to axis in 12a

page 18, Figure 19 caption corrected spelling of 'reference'

page 20, Figure 21 caption added apostrophe to 'bird's-eye view'

page 23, Figure 23, removed t and s from (b) and made font uniform in labels of (c)

page 25, reworded first paragraph of Section 8

page 39, Figure 38 caption added a space between 'overlying' and 'Aztec'

page 42, Figure 42 caption changed from 'by yellow' to 'in yellow'

page 44, last sentence of first paragraph changed 'provided' to 'listed'

page 59, second paragraph of Box 3 changed 'As shown in Figure 42b and its inset, groundwater levels' to 'As shown in Figure 42c, groundwater levels'

pages 65 and 68, added Dr. before author names where it was missing for Aydin, Antonellini, Deng, and Joussineau

Changes from the Version 2 to Version 3

Version 3: 30 January 2023

Page numbers refer to page numbers in the pdf of Version 2

<u>Specific changes:</u>

page ii, updated version number and date

page 1, 1st paragraph, 7th line, removed the word 'formation' from before the word 'mechanisms'

page 8, replaced Figure 9 with a better layout